



Pergamon

Progress in Oceanography 41 (1998) 455–504

Progress in Oceanography

The transition zone of the Canary Current upwelling region

E.D. Barton^{a,*}, J. Arístegui^b, P. Tett^c, M. Cantón^d,
J. García-Braun^e, S. Hernández-León^b, L. Nykjaer^f,
C. Almeida^b, J. Almunia^b, S. Ballesteros^b, G. Basterretxea^b,
J. Escánez^g, L. García-Weill^b, A. Hernández-Guerra^b,
F. López-Laatzen^g, R. Molina^g, M.F. Montero^b,
E. Navarro-Pérez^a, J.M. Rodríguez^g, K. van Lenning^b,
H. Vélez^a, K. Wild^a

^aSchool of Ocean Sciences, University of Wales, Bangor, Wales, UK

^bFacultad de Ciencias del Mar, Universidad de Las Palmas de Gran Canaria, Spain

^cDepartment of Biological Sciences, Napier University, Edinburgh, Scotland, UK

^dUniversidad de Almería, Spain

^eUniversidad de La Laguna, Tenerife, Spain

^fJoint Research Centre, Ispra, Italy

^gCentro Oceanográfico de Canarias, Instituto Español de Oceanografía, Tenerife, Spain

Abstract

Like all the major upwelling regions, the Canary Current is characterised by intense meso-scale structure in the transition zone between the cool, nutrient-rich waters of the coastal upwelling regime and the warmer, oligotrophic waters of the open ocean. The Canary Island archipelago, which straddles the transition, introduces a second source of variability by perturbing the general southwestward flow of both ocean currents and Trade winds. The combined effects of the flow disturbance and the eddying and meandering of the boundary between upwelled and oceanic waters produce a complex pattern of regional variability. On the basis of historical data and a series of interdisciplinary field studies, the principal features of the region are described. These include a prominent upwelling filament originating near 28°N off the African coast, cyclonic and anti-cyclonic eddies downstream of the archipelago, and warm wake regions protected from the Trade winds by the high volcanic peaks of the islands. The filament is shown to be a recurrent feature, apparently arising from the interaction of a topographically trapped cyclonic eddy with the outer edge of the coastal upwelling zone. Its role

* Corresponding author.

in the transport and exchange of biogenic material, including fish larvae, is considered. Strong cyclonic eddies, observed throughout the year, drift slowly southwestward from Gran Canaria. One sampled in late summer was characterised by large vertical isopycnal displacements, apparent surface divergence and strong upwelling, producing a fourfold increase in chlorophyll concentrations over background values. Such intense eddies can be responsible for a major contribution to the vertical flux of nitrogen. The lee region of Gran Canaria is shown to be a location of strong pycnocline deformation resulting from Ekman pumping on the wind shear boundaries, which may contribute to the eddy formation process. © 1998 Elsevier Science Ltd. All rights reserved.

Contents

1. Introduction	456
2. Data	458
3. Large scale context	460
3.1. Seasonal variation	460
3.2. Regional variation	466
4. Mesoscale variability	468
4.1. Upwelling filaments	469
4.2. Island eddies	482
4.3. Island lee	490
5. Discussion	492
6. Acknowledgements	501
7. References	501

1. Introduction

In recent years the richness of mesoscale structure associated with upwelling areas has been revealed by the use of satellite observations of sea surface temperature patterns and ocean colour (Traganza, Nestor, & McDonald, 1980). The interaction between the coastal upwelling regime over the continental shelf and the offshore oceanic regime has been shown to be highly variable and to take place in a zone several hundred kilometres wide. The boundary between the cool, nutrient-rich upwelled waters and the warmer, nutrient-poor offshore waters is irregular and often contorted to form long, narrow, offshore-flowing streamers or filaments of upwelled water which may reach far offshore. Much effort has been expended on examining these features typical of the 'Coastal Transition Zones' in terms of their in situ characteristics and role in shelf–ocean exchange of biota and nutrients (Brink, & Cowles, 1991). Filaments appear to arise from more than one cause, however, and may differ between sites and regions (Strub, Kosro, & Huyer, 1991).

The northwest African upwelling region is typical in terms of the obvious presence of filaments (Van Camp, Nykjaer, Mittelstaedt, & Schlittenhardt, 1991), though so far they have been little studied there. It differs from other upwelling zones because

of the presence of the Canary Islands, which provide another major source of meso-scale activity (Arístegui, Sangrá, Hernández-León, Cantón, Hernández-Guerra, & Kerling, 1994; Arístegui, Tett, Hernández-Guerra, Basterretxea, Montero, Wild, Sangrá, Hernández-León, Cantón, García Braun, Pacheco, & Barton, 1997). The archipelago consists of seven main islands distributed zonally across the eastern limb of the subtropical gyre of the North Atlantic at a latitude near 28°N (Fig. 1). The volcanic islands rise steeply from sea floor depths in excess of 2000 m with deep

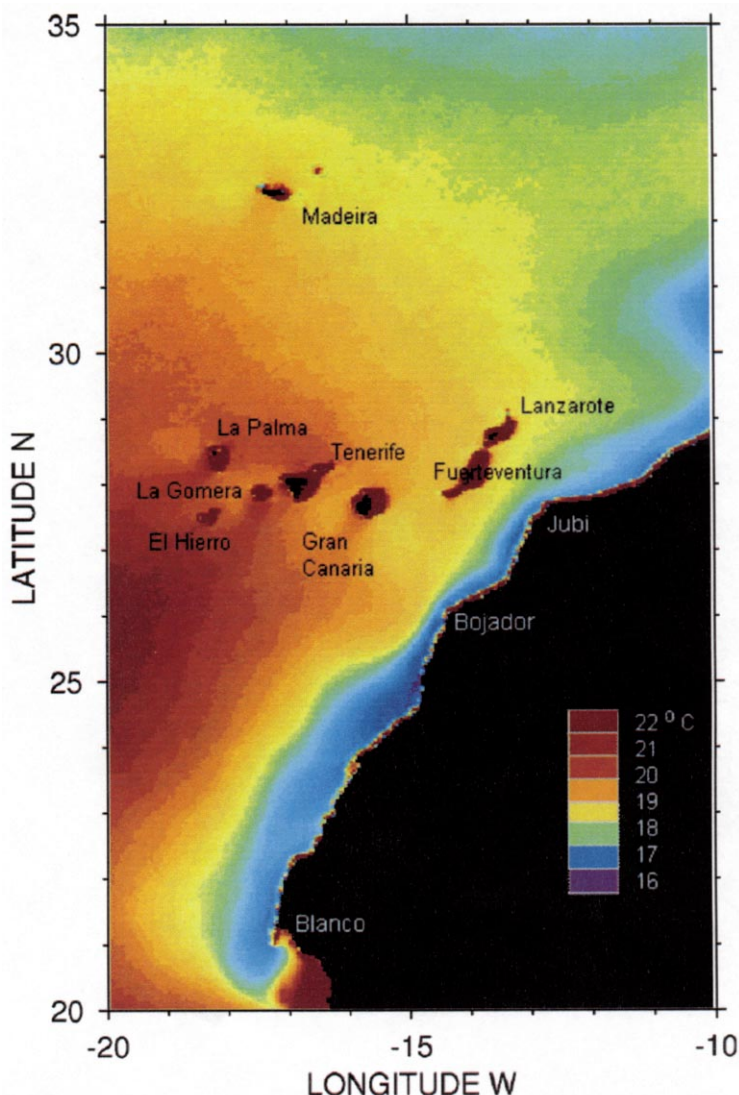


Fig. 1. Long term (1981–1991) mean sea surface temperature derived from Global Area Coverage AVHRR data.

channels separating them. Their summits reach a maximum height of 3718 m on Tenerife, where Teide is the highest mountain in all Spain. Fuerteventura is separated by a distance of some 90 km from the African mainland coast, and the archipelago extends some 400 km further west. The islands thus span the transitional zone linking the continental shelf upwelling region of northwest Africa to the open ocean waters of the subtropical gyre. They present a barrier to both the weak equatorward flow of the Canary Current and to the flow generated by the Trade winds, thus giving rise to a variety of mesoscale phenomena.

Early studies described the Canary region as ‘oligotrophic’, comparable to the open ocean subtropical gyres (De León, & Braun, 1973; Braun, 1980). However, this general view has changed during recent years, following the analyses of sea-surface temperature and chlorophyll derived from satellite images, and the study of physical and biological data gathered during shipboard sampling of the mesoscale variability of the region.

In this paper we discuss the results of a recent inter-disciplinary European project to study the Canary Island region in terms of its annual cycle and the various sources of mesoscale variability. The work is based on data collected during a series of three cruises carried out in different seasons, and supplemented by archived data from a variety of sources. The cruises had different individual emphases but all three sampled a dense grid south of Gran Canaria to study island wakes and eddies, two measured conditions along transects across the entire archipelago, and one made intensive measurements between the islands and the African coast to sample an upwelling filament (Fig. 2). Notionally the area can be divided into four sub-regions, waters north of the archipelago, affected (1) and unaffected (2) by the NW African coastal upwelling system; and southern waters, perturbed after flowing through the islands chain, affected (3) and unaffected (4) by the African upwelling. As will become apparent, the upwelling-open ocean boundary is contorted and subject to significant variability. This region affected by the boundary, constitutes the transition zone.

We provide an up-to-date overview of the area as a basis for more specialised reports and process studies in preparation, to document in some detail the major processes influencing mesoscale activity and to evaluate the importance of those processes. This zone of transition between coastal upwelling and open ocean conditions is important not only for its regional significance (for example in supporting a fishery through enhanced primary production), but also because it provides a convenient site for the study of two globally important processes. These are: (1) shelf-ocean exchange associated with eastern boundary upwelling; and (2) the disproportionate contribution of continental margin and island stirring to horizontal and upper-ocean vertical mixing in the subtropical ocean gyres. ‘Mesoscale activity’ is another way of labelling this stirring and its immediate consequences.

2. Data

Field data were obtained during three cruises on board R.V. *García del Cid*, 9–17 March 1991, on R.V. *Ignat Pavlyuchenkov*, 25 October–25 November 1991 and

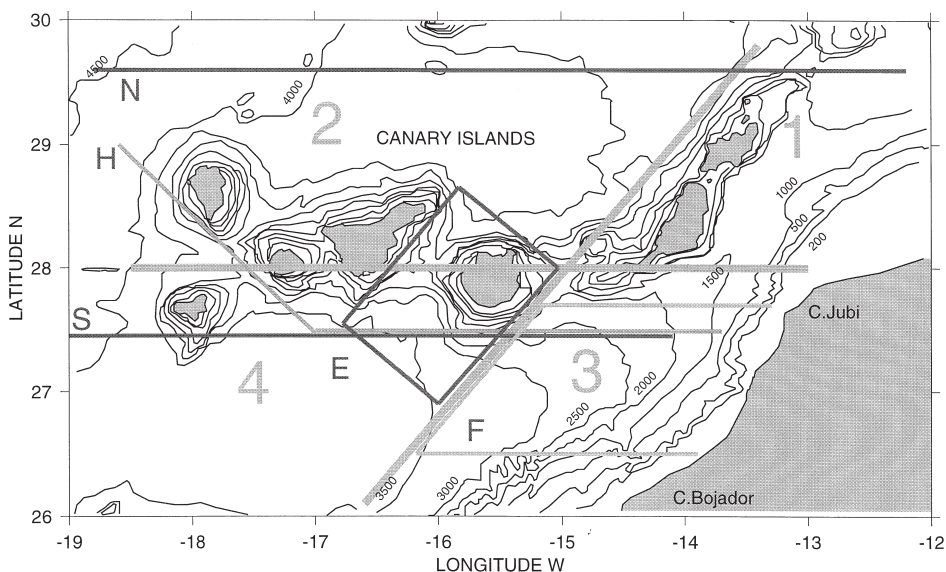


Fig. 2. Canary Islands region showing study areas for eddy surveys (E), filament survey (F) and long sections (N and S in October 1991 and H in August 1993). The region can conceptually divided into four zones of influence: (1) dominated by coastal upwelling, (2) undisturbed oceanic, (3) upwelling and island influenced and (4) oceanic island influenced. Depth contours are marked in metres.

on R.V. *Hespérides*, 5–26 August 1993. The cruises took place during the three representative phases of the seasonal development of production in the Canaries region. These are: (1) the end of the winter period, when a bloom takes place; (2) the strongest Trade wind period, when coastal upwelling is most developed; and (3) early autumn, when winds are weakest and stratification is strongest. Wind data were obtained from the airport on the exposed east coast of Gran Canaria supplied by the Spanish Instituto Nacional de Meteorología.

Cruise observations consisted of interdisciplinary surveys as represented in Fig. 2. Each cruise included a grid of about 50 Conductivity-Temperature-Depth (CTD) stations at roughly 20 km spacing around Gran Canaria to observe island-induced eddies and other downstream effects (Box E). The October–November cruise included the two zonal transects (N and S) of stations at 20 km intervals to compare conditions upstream and downstream of the archipelago. The August cruise resampled most of transect S and a line extending northwest between the outer islands (Line H). Additionally this cruise made a survey of the northwest African coastal upwelling between Cabo Jubi, Cabo Bojador and 200 km offshore. Data were gathered with a SeaBird SB-19 CTD probe in the first cruise (Arístegui, Tett, Hernández-Guerra, Basterretxea, Montero, Wild, Sangrá, Hernández-León, Cantón, García Braun, Pacheco, & Barton, 1997), with a Niel Brown Mk III in the second cruise (Vélez-Muñoz, 1992) and with a SeaBird SB9-11 + probe in the August 1993 cruise (Navarro-Pérez, Vélez-Muñoz, & Wild, 1994). Casts were made generally to 600 m

or the sea bed, where shallower, though some were made to 1000 m. Ship board ADCP (Acoustic Doppler Current Profiler) observations made from the R.V. *Hespérides* in August 1993 are reported by Navarro-Pérez, & Barton (1995).

At many stations other variables were sampled with additional sensors and Niskin bottles on the CTD rosette, with separate bottle casts and with assorted net hauls. Properties determined included chlorophyll-*a* (Wild, 1992; Navarro-Pérez, Vélez-Muñoz, & Wild, 1994), oxygen and nutrients (Braun, & Escánez, 1996), primary production (Basterretxea, 1994), Electron Transport System activity in microplankton (Montero, 1992), phytoplankton and bacteria (Wild, 1995; Ballesteros, 1992; Kennaway, & Tett, 1994), zooplankton biomass (Hernández-León, 1988) and fish larvae (Rodríguez, 1996).

Sea Surface Temperature (SST) images were obtained from High Resolution Picture Transmission (HRPT) data from the Advanced Very High Resolution Radiometer (AVHRR) sensors onboard the National Oceanic and Atmospheric Administration (NOAA) satellites. A split window algorithm designed by Castagné, Le Borgne, Le Vourch, & Olry (1986) was used to correct for atmospheric water vapour. SST is calculated with an accuracy of about 0.5°C by this algorithm (Le Borgne, Le Vourch, & Marsouin, 1988). The images were plotted on a Mercator Projection with a 1 km pixel resolution.

3. Large scale context

3.1. Seasonal variation

In the North Atlantic throughout most of their meridional extent the Trade winds have a strong alongshore component which drives upwelling at the eastern boundary. The large scale upwelling is seen in mean sea surface temperature fields for the years 1981–1991 derived from AVHRR Global Area Coverage data (4 km resolution) from the NOAA satellites (Fig. 1). The overall isotherm pattern reflects the form of the eastern limb of the subtropical gyre. Lower mean temperatures occur in a coastal boundary zone that includes at least the inner Canary Islands. The southern limit of the year round upwelling is seen at Cabo Blanco. A disturbance effect by the islands is evident even in this long term mean picture, in which regions of higher temperature form wake-like patterns southwest of the five outer islands and to a lesser extent the inner two.

Wooster, Bakun, & McLain (1976); Speth, Detlefsen, & Sierts (1978); Nykjaer, & Van Camp (1994) have shown that during the months of June to September the Trade wind band affects the African coast between about 35°N and 20°N and have demonstrated the strong relation between the coastal temperature anomaly with respect to mid-ocean and the Ekman transport normal to the coast. In November to April the Trades, located further south in response to the southward shift and strengthening of the Azores High–Saharan Low system, affect the coast between about 30°N and 12°N. This annual cycle is manifest in the locality of the Canaries as a variation in strength and orientation of the Trade winds, leading to a strong

annual rhythm in wind forcing. In contrast to temperate latitudes, however, the strongest wind forcing is in the boreal summer, at about the same time as the strongest heating.

The annual march of sea surface temperature, wind vectors and estimated Ekman transport for latitude 29°N from the African coast to west of the Canaries is shown in Fig. 3. Monthly means of all available data from COADS, the Comprehensive Ocean-Atmosphere Data Set (Roy, & Mendelsohn, 1995), are shown for one degree squares. Ekman transport is calculated from the monthly mean wind stresses. The intensification of winds is evident between June and September as their direction changes from northeasterly to northerly. At these latitudes the monthly mean winds blow with an equatorward component along the African coast year round with the peak intensity occurring in July–August. The accompanying strengthening of the zonal temperature gradient is also clear. Maximum temperature contrast between coast and 20°W is seen in August–September. The latter is largely a result of the strengthening of the increased upwelling during summer at the African coast, though surface temperatures increase generally because of summertime insolation and heat gain by the ocean. Conditions are upwelling favourable throughout the year therefore, though less so in the winter months when the winds are weakest and most variable in direction. The strongest nearshore cooling is not revealed by the 1 degree grid resolution of this data set.

Realisations of the mean fields of sea surface wind, Ekman transport and temperature for the seasons corresponding to the project cruises show the major geographic and annual variation (Fig. 4). The intensity of the monthly mean winds increases significantly during the summer (August) throughout the area, although they remain conducive to upwelling in all months. The winds are weakest in November but are almost as weak in March. The general form of the temperature field shows that the typical cooler region of upwelling near the African coast persists year round. The southern limit of the upwelling in summer is clearly seen at Cabo Blanco (20° 50' N). A striking difference between the summer and other periods is that the isotherms show a weaker meridional temperature gradient across and north of the Canaries in August. During the other seasons they lie almost zonally, but in summer they trend northwest to southeast. This change represents the large scale seasonal alteration of the shape and location of the eastern limb of the subtropical gyre reported by Stramma, & Siedler (1988).

The mean Ekman transport (Fig. 4) shows significant zonal and meridional gradients, which decrease generally from the coast towards open ocean and from south to north. The wind stress curl and hence the vertical velocity at the base of the Ekman layer were calculated at 1° intervals by a centred difference scheme from the COADS pseudo-stress data. Sources of error in such calculations are discussed by Bakun, & Nelson (1991). The upwelling velocity, shown as contours overlaid on the wind stress maps in Fig. 4, shows the Ekman layer is divergent within 100–150 km of the African coast. This indicates an upward velocity and implies upwelling occurs year round as suggested by the temperature distributions. The temperature contours tend to parallel the coast within the region of divergence. Maximum values of estimated monthly mean upwelling velocity were around 0.4 m d⁻¹, but the diver-

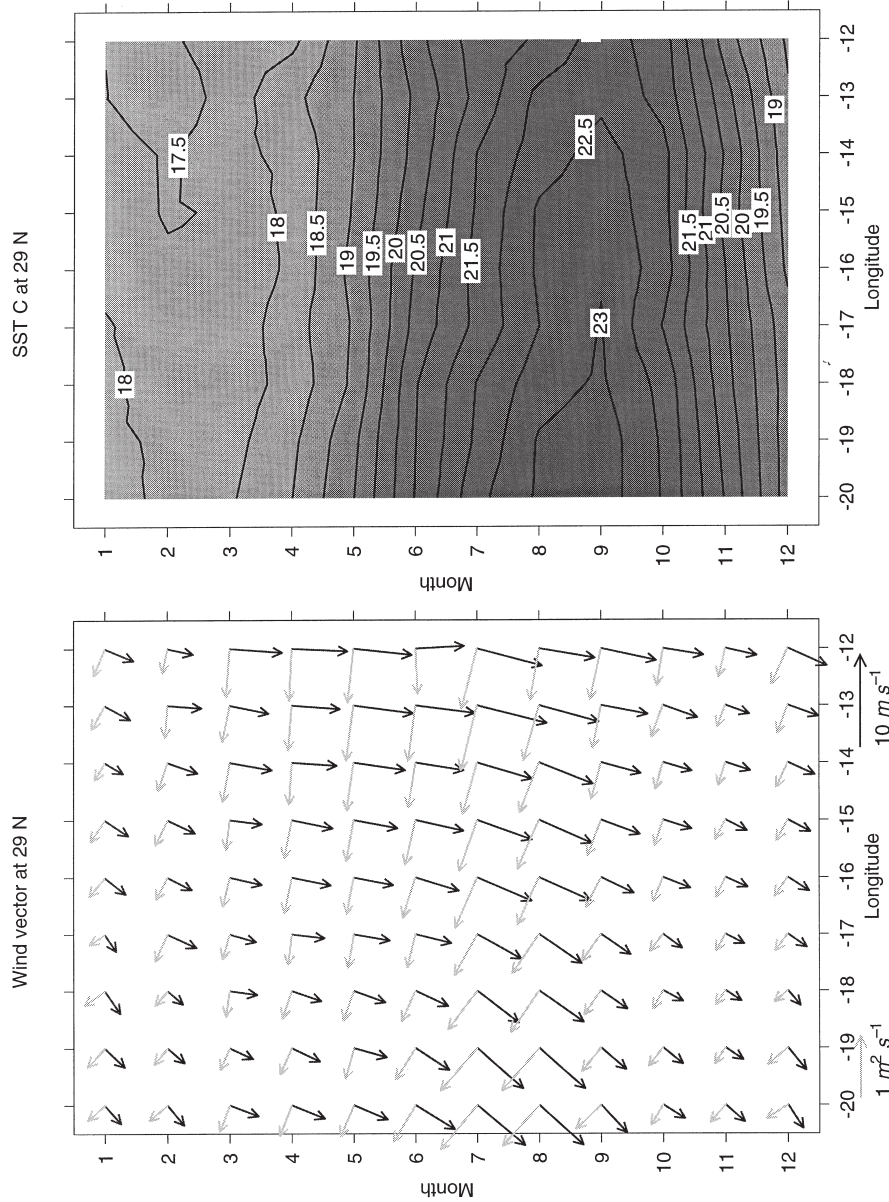


Fig. 3. Annual cycle of monthly mean sea surface temperature (°C) and wind vectors at 29°N. Lighter arrows indicate the Ekman transport vector calculated from the mean monthly wind stress.

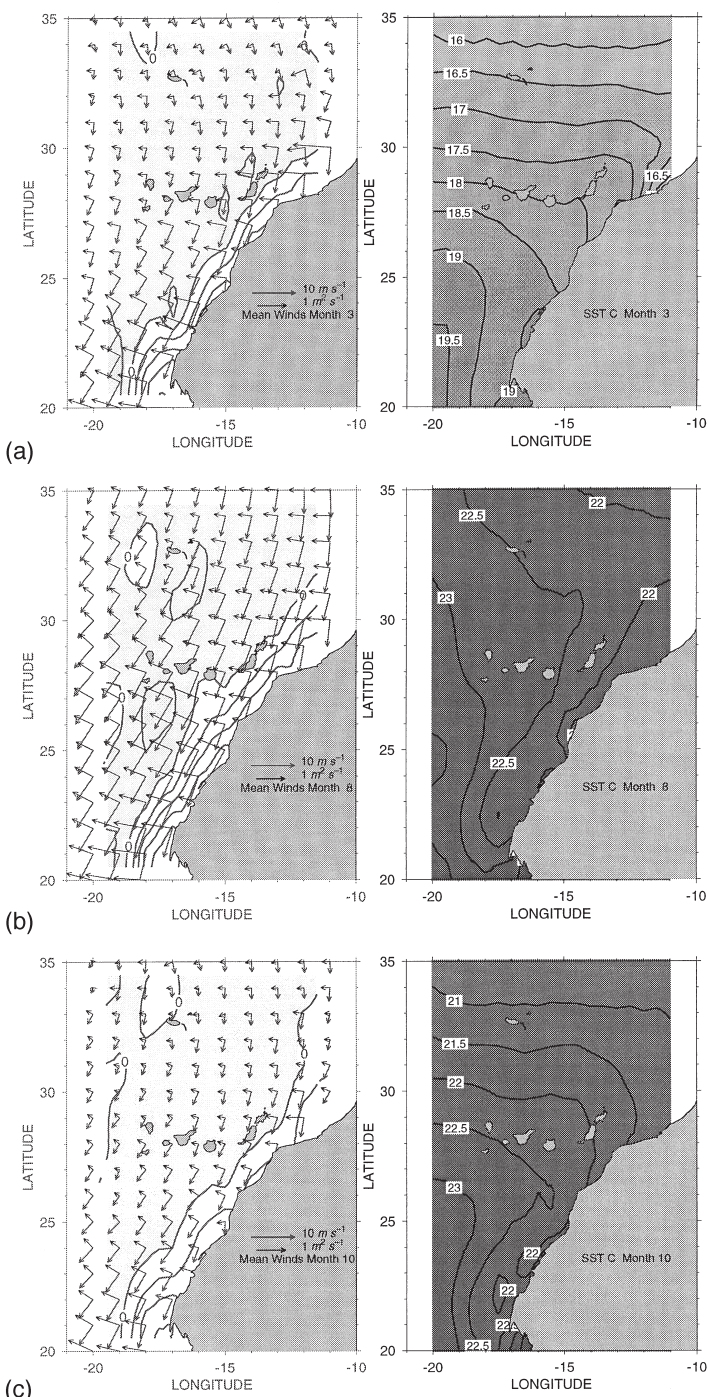


Fig. 4. Maps of monthly mean surface wind velocity, Ekman transport and upwelling velocity (left) and sea surface temperature (right) for (a) March (b) August (c) October. Contours of vertical velocity are at 0.1 m d^{-1} intervals; negative values (downwelling) are shaded.

gence is under-estimated at the coast because of the 1° spacing of the observation grid. In the offshore area the field is weakly convergent. The position of the zero vertical velocity contour varies with season, but provides a basis for locating the hypothetical boundary between upwelling affected areas (1) and (3) and oceanic conditions of areas (2) and (4) indicated in Fig. 2.

The mean annual cycle of temperature in waters to the north-west of the Canaries archipelago is shown in Fig. 5. This exemplifies the seasonal and depth variation of hydrographic structure in the undisturbed and oligotrophic oceanic waters of the Canary Current. The data are monthly averaged values for the area 4 ($29\text{--}31^{\circ}\text{N}$, $17\text{--}19^{\circ}\text{W}$) calculated from the National Oceanic Data Center archive. The period of strongest near surface stratification occurs in June to October when not only insolation, but also wind forcing, are strongest. The situation differs from the temperate seas where winter cooling coincides with strong winds. Nevertheless, convection resulting from surface cooling and aided by wind stirring during winter, is sufficient

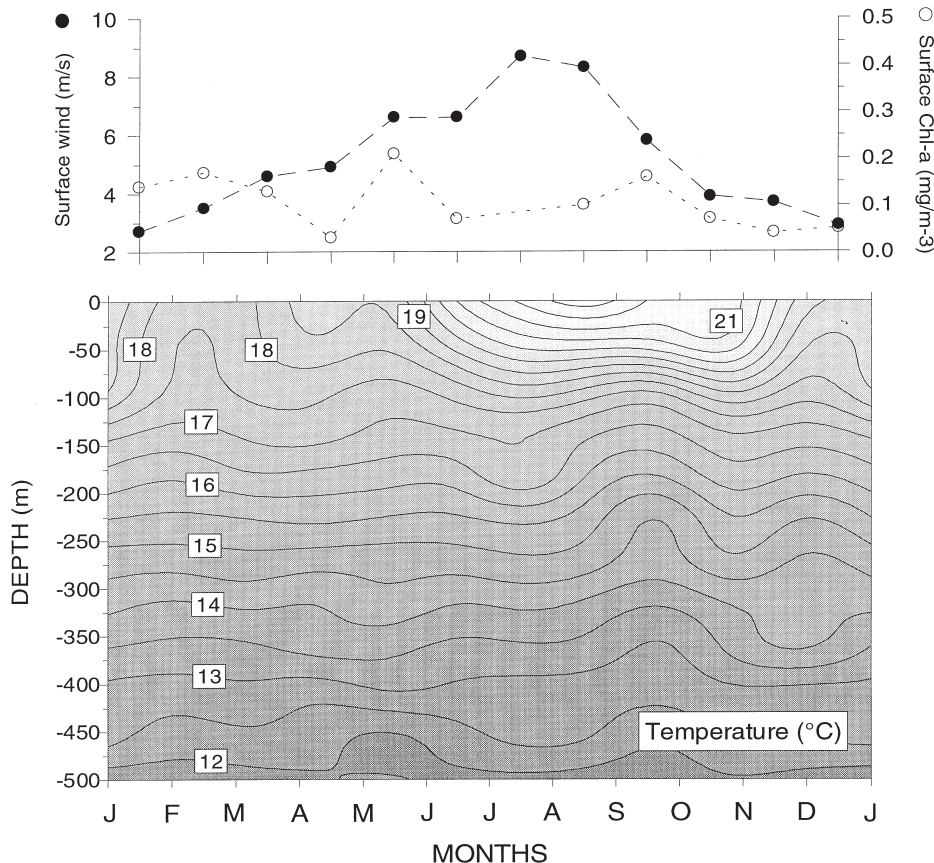


Fig. 5. Annual cycle of temperature, integrated chlorophyll and surface wind in the oceanic region unperturbed by island or upwelling.

to weaken the seasonal stratification from November on. The time of maximum penetration of the surface mixed layer (~ 100 m) is February to April. The seasonal thermocline begins to reform in April–May and reaches its greatest intensity, when surface temperatures are highest in August–September, despite the maximum winds occurring in August.

Detailed seasonal biological studies of the Canaries region are few but it is reported that mean chlorophyll concentrations are low ($< 0.5 \text{ mg Chl m}^{-3}$) for most of the year (Arístegui, Hernández-León, Gómez, Medina, Ojeda, & Torres, 1989; Arístegui, Tett, Hernández-Guerra, Basterretxea, Montero, Wild, Sangrá, Hernández-León, Cantón, García Braun, Pacheco, & Barton, 1997). Mean monthly surface values compiled from these sources, shown in Fig. 5 for the area northwest of the islands, indicate only slight enhancement at the end of winter. Chlorophyll values up to 1 mg m^{-3} have been reported close to the islands (Braun, Orzaiz, Armas, & Real, 1985), although these concentrations were probably enhanced by local oceanographic processes.

The annual production cycle in Canaries waters unaffected by the NW African coastal upwelling can be broadly divided into three periods: (1) the late winter bloom, when the seasonal thermocline is eroded and nutrients from deeper layers are mixed up into the previously depleted surface waters; (2) the summer season, which corresponds with the period of highest trade winds intensity, and therefore of high coastal upwelling activity; and (3) the autumn season, when wind intensity decreases, the seasonal stratification is at its most intense and plankton productivity falls to its lowest annual values. The dynamics of the winter bloom are more similar to those of the autumn (nutrient-limited) rather than the spring (light-limited) bloom of temperate seas.

From late spring to early winter, the period of superficial stratification, most chlorophyll is found in a deep maximum (DCM) within the seasonal thermocline. Picophytoplankton ($< 2 \mu\text{m}$) are the most typical photosynthetic organisms, contributing to chlorophyll and production with $> 75\%$ in autumn and up to 50% in spring (Montero, 1993). Smaller phytoflagellates dominate the DCM, whereas cyanobacteria are most abundant in the surface mixed layer or SML (Ballesteros, 1994). Phytoplankton larger than $2 \mu\text{m}$ are scarce during most of the year, except in the African coastal upwelling zone, where diatoms are abundant.

The relatively small year round variation in chlorophyll concentrations integrated over the water column (approximately between $15\text{--}60 \text{ mg Chl m}^{-2}$) contrasts with the much larger variability in primary production values. During the autumn, primary production is as low as in the most oligotrophic regions of the world ($25\text{--}30 \text{ mg C m}^{-2} \text{ d}^{-1}$; Li, 1994; Basterretxea, 1994). In late winter and early spring, however, productivity values increase more than an order of magnitude (up to $1000 \text{ mg C m}^{-2} \text{ d}^{-1}$). Even values higher may occur associated with distinct mesoscale features (like eddies and fronts) which produce upwelling of deep nutrient-rich water into the surface waters.

The seasonal increase in primary productivity is not accompanied by a similar increase in chlorophyll accumulation. The study of the available in situ chlorophyll data together with the complete archive of CZCS images in the Canaries region,

indicates that at the start of the mixing period (January–February) only a weak bloom is produced. It appears that grazers take advantage of the phytoplankton bloom rapidly to prevent any surface accumulation (Aristegui, 1990), so that the bloom never has time to build up and then weakens into spring and summer (Braun, Orzaiz, Armas, & Real, 1985). Zooplankton biomass reaches its maximum a few weeks after the phytoplankton peak, and drops sharply as the algal standing crop falls (Hernández-León, 1988). Additional zooplankton peaks have been described during late spring and summer in the wakes of the islands coinciding with strong wind pulses (Hernández-León, 1991). CZCS images show that highest chlorophyll concentrations occurring at the sea surface in the northwest African upwelling region in July–August (Hill, Hickey, Shillington, Strub, Brink, Barton, & Thomas, 1997); highest primary production values we observed were in the upwelling region near Cabo Bojador during the August 1993 cruise.

3.2. Regional variation

Conditions upstream (sub-regions 1 and 2 of Fig. 2) and downstream of the islands (sub-regions 3 and 4) were compared during the cruise carried out in October–November 1991 on board the R/V *Ignat Pavlyuchenkov*. A major goal of the cruise was to look for evidence of increased biological productivity in the wake downstream of the island. Calm seas and strong surface heating typified this period, and winds were even weaker than expected at this time of year. The surface heating reduced sea surface temperature gradients across the area of interest, and the persistent cloudiness prevented acquisition of very many useful satellite images.

Although the sampling period corresponded to the season of lower productivity, lower influence of the African upwelling and higher stratification of the water column, the four Canary region sub-divisions (Fig. 2) were still distinguishable by both their physical and biological properties. The long zonal section made north of the islands was quite uniform in temperature, salinity and chlorophyll-a, typical of the far field, except in the upwelling region near to the African coast (Fig. 6). Whereas a parallel section to the south presented significant perturbations and eddy-like structures, presumably caused by the islands. Comparisons between the sections showed that the southern section was significantly more variable in terms of isotherm excursions and presented a shallower DCM. Chlorophyll integrated over the 0–200m layer was higher in the southern section (Fig. 7), where the nutricline was shallower (Fig. 8). In both sections chlorophyll concentrations (Figs. 6 and 7) and abundances of cyanobacteria and phytoflagellate cells (Fig. 8) were higher in the eastern stations, providing evidence of the upwelling influence. The boundary between the coastal upwelling zone and offshore waters was strongly demarcated between stations 17 and 18, southeast of Gran Canaria (Fig. 6). The mean primary production values in the mixed layer in the southern section (Fig. 7) show a clear influence of a cyclonic eddy at stations 19 and 20 (presumably originating from Gran Canaria). This influence is not so clearly visible in the integrated chlorophyll field. In all instances average chlorophyll concentrations were very low at this time of the year, as was to be expected from the strong stratification.

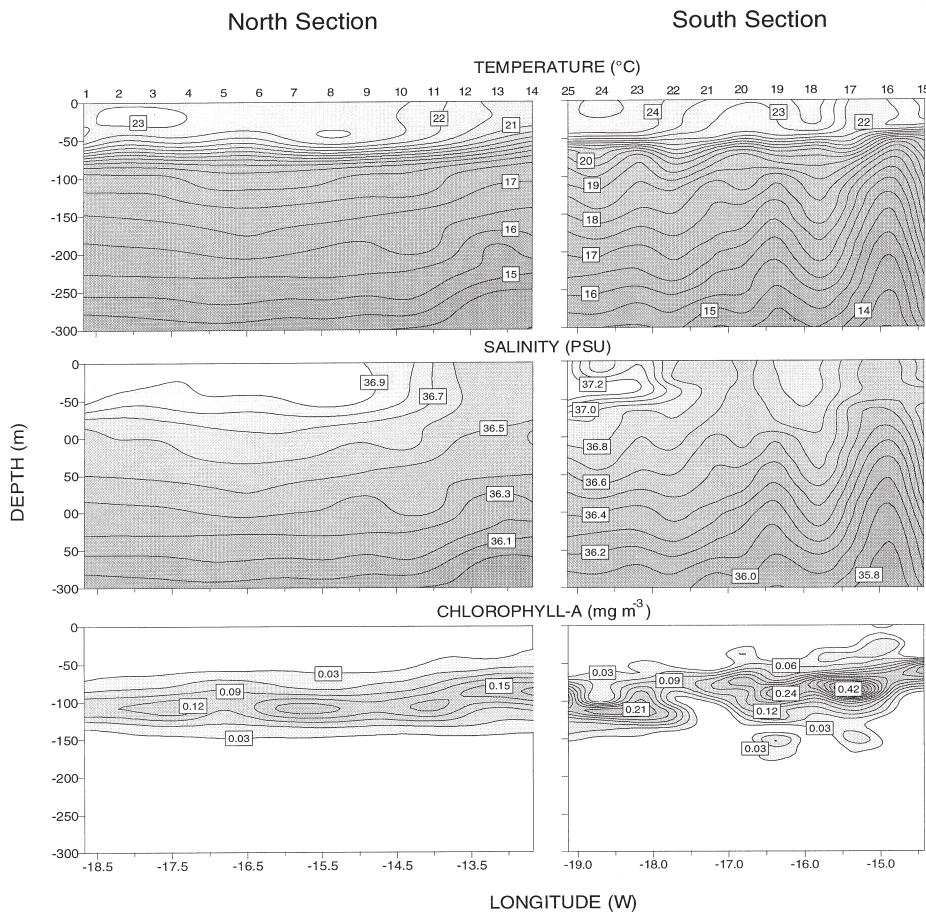


Fig. 6. Sections of temperature, salinity and chlorophyll-a north and south of Canary Islands in October 1991 (Lines N and S in Fig. 2) show the effects of the African upwelling in the east and island perturbations on the southern section.

Evidence of upstream-downstream differences across the archipelago was supported by comparisons of two 24-hour time series made north and south of Gran Canaria in October 1991. At the southern station, close to a cyclonic eddy, the DCM was shallower and more intense although the pycnocline on this occasion was only slightly shallower (Fig. 9). The mean depth of the nutricline was about 30 m shallower and the mean water-column integrated chlorophyll about double that in the far field, at the northern station (Fig. 10). Furthermore, microbial respiration (expressed as ETS activity) was significantly higher in the southern station. While variability between individual stations can occur as a result of patchiness of open ocean phytoplankton on scales of kilometers, the persistent difference between the time series stations and more generally between the northern and southern lines indi-

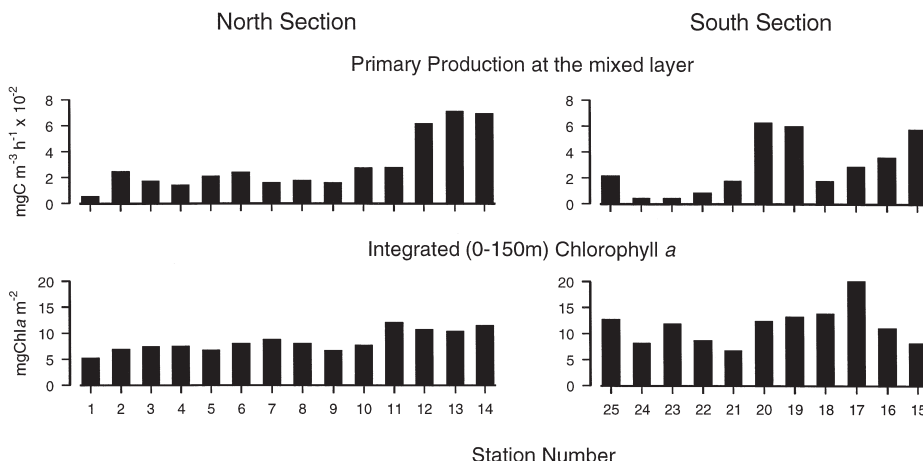


Fig. 7. Horizontal profiles of primary production in the mixed layer and chlorophyll integrated from 0–150 m along the sections north and south of the Canary Islands in October 1991.

cate variability at somewhat larger scales. These results are evidence that there was an island mass effect caused by the archipelago perturbing the mean flow.

4. Mesoscale variability

Recent satellite and field observations have revealed that there is strong year-round mesoscale variability in both temperature and chlorophyll distributions in the waters of the archipelago that is superimposed on the background seasonal and regional variation (Arístegui, Sangrá, Hernández-León, Cantón, Hernández-Guerra, & Kerling, 1994; Arístegui, Tett, Hernández-Guerra, Basterretxea, Montero, Wild, Sangrá, Hernández-León, Cantón, García Braun, Pacheco, & Barton, 1997). By mesoscale, we refer to the range of phenomena whose dominant spatial scale lies between approximately one and ten times the baroclinic Rossby radius, with a concomitant temporal scale of one to ten inertial periods. This encompasses the approximate ranges of 10 to several hundred kilometres and time periods of one day to several weeks. Much of this variation is associated with eddies and other island effects, and with the intrusion of cold, chlorophyll-rich coastal upwelling waters westward into the area of the eastern islands. Substantial mesoscale variability was evident during all three cruises. The variability included both cold-core, cyclonic, eddies, as seen during all cruises, and also warm-core, anticyclonic, eddies, as seen during the March 1991 cruise. The eddies sampled during the cruises lay to the south and south-west of Gran Canaria, as would be expected if they resulted from flow perturbations by the island. Regions of colder and less saline water, evidence of the offshore limits of a filament, were seen to the southeast of Gran Canaria during the cruises in March and October 1991, while in August 1993, a clearly defined upwelling filament, which ended in a cyclonic eddy southeast of Gran Canaria was thoroughly studied.

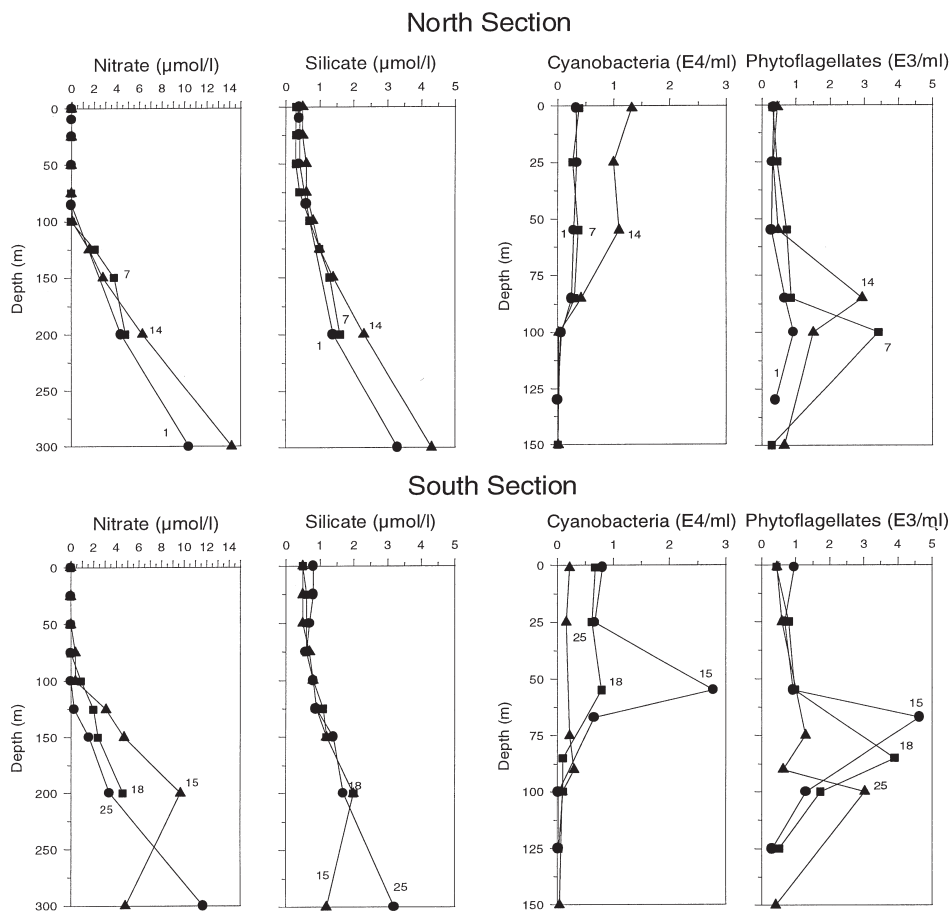


Fig. 8. Vertical profiles of nitrate, silicate, cyanobacteria and phytoplankton at selected stations in the sections north and south of the Canary Islands in October 1991.

4.1. Upwelling filaments

As shown by AVHRR and CZCS (Coastal Zone Color Scanner) imagery, the southeastern Canary region is frequently invaded by upwelling waters arriving in the form of narrow cold chlorophyll-rich filaments extending some hundred kilometres offshore. A detailed study of one of these recurrent features was carried out in August 1993, during the season when, according to the climatic average data, upwelling was strongest. Winds were so strong during the cruise that sampling had to be abandoned for a time because of the sea state. However, as the result of this strong forcing, many well-developed mesoscale features were evident in the area, and were well-sampled.

Atmospheric conditions were clear on a number of days during the cruise and wind mixing prevented significant surface heating from obscuring near-surface temperature patterns. Five images reveal that the filament persisted between 2 and 29

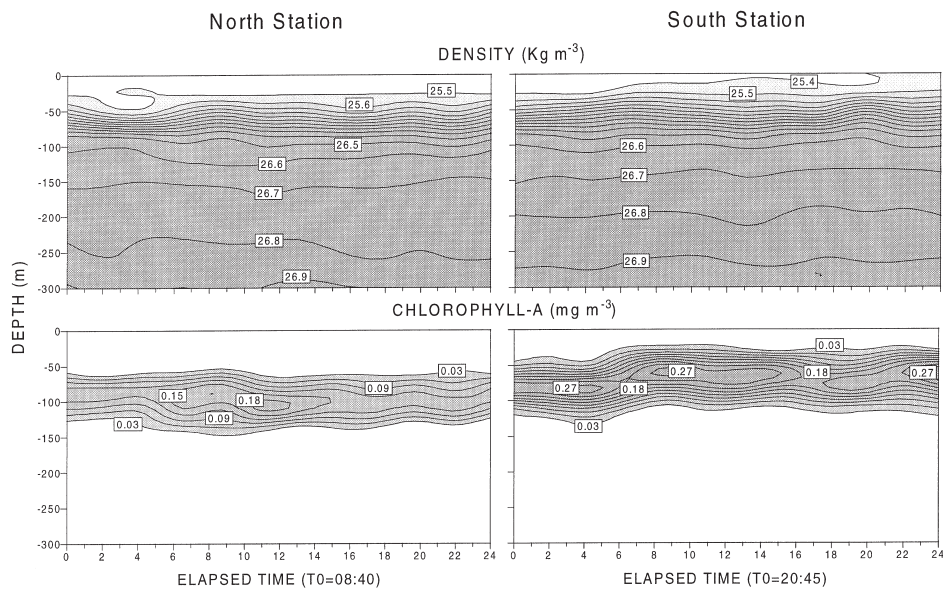


Fig. 9. Time series from two stations north and south of the Canary Islands showing profiles of density anomaly and phytoplankton in October 1991.

August 1993 (Fig. 11a to e). The filament appeared to arise on the continental shelf near 27°N, just north of Cabo Bojador. It extended over 150 km northwest towards Gran Canaria but appeared to be diverted cyclonically to the south in the early images of 2 and 4 August. The development of the filament was related to the winds (Fig. 11f). Following the start of the cruise on 4 August there was a period of strong winds which briefly exceeded 25 m s⁻¹ on 7 August. (In the record apparent wind reversals occur where the ship passed through the lee of the islands.) By 10 August the cyclonic formation appeared more clearly and the filament itself was more sharply delineated as an extended narrow tongue of cooler water of 21.5–22°C wrapped around a slightly warmer core. The structure was still present through 18 August, though on that day its detailed configuration was obscured by cloud. After 18 August the winds relaxed considerably and by 29 August, after the end of the cruise, the filament was still clearly visible but less strongly defined. Generally the coastal upwelling seemed to be constrained well within the width of the continental shelf, as defined by the 200 m contour. However, on 10 and 18 August it had expanded to the shelf limit almost everywhere in the region as a result of the wind strength. The filament's width was generally about 20 km or less and it was bounded by strong temperature gradients to both north and south. Coastal upwelling, and the filament temperature contrast, appeared weaker on 4 and 29 August.

The position of the filament's base near to the shore varied little (Fig. 11) except in the image of 18 August, which may have been affected by cloud contamination. Statistical studies of filaments off the western coast of Iberia shows that they frequently arise slightly downstream of particular coastal features such as capes

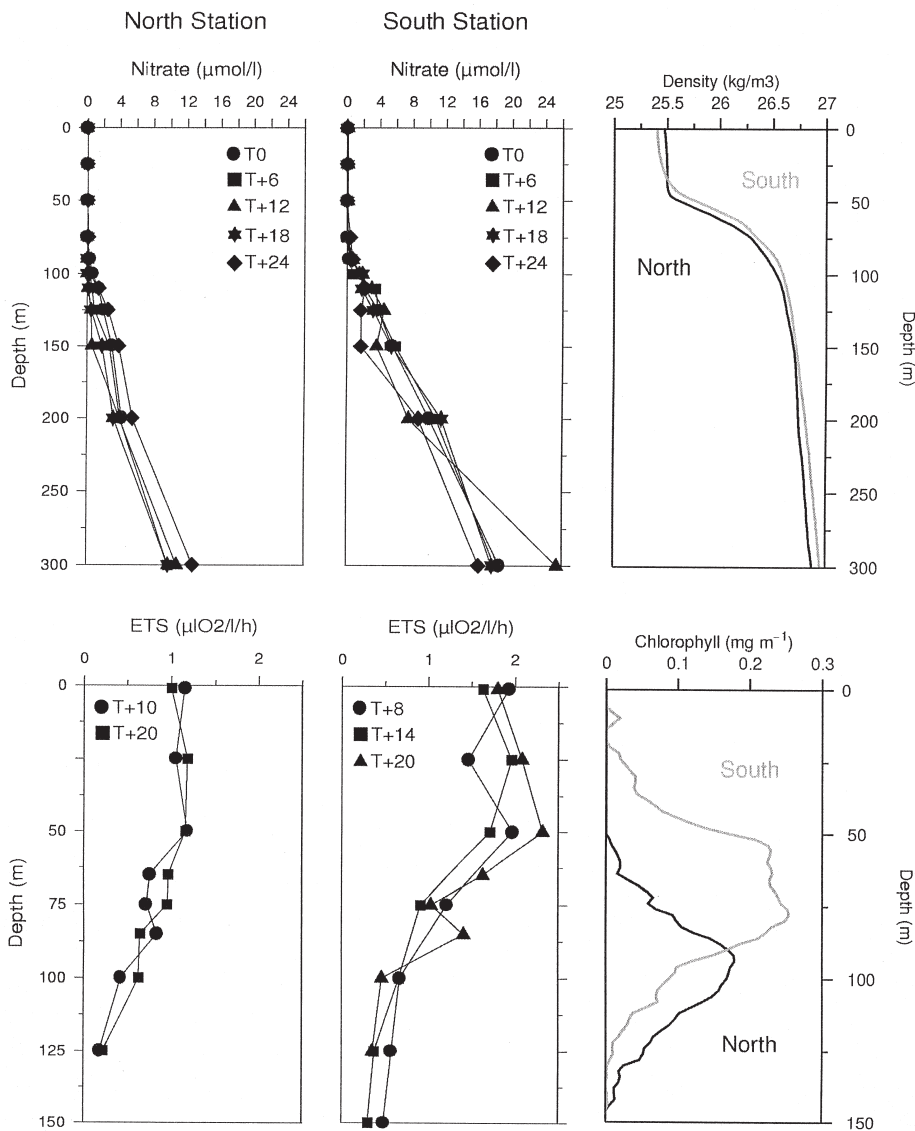


Fig. 10. Vertical profiles of nitrate, ETS activity in microplankton, density and chlorophyll at the 24 hour time series stations north and south of the Canary Islands in October 1991. Times of individual profiles shown are given as T + 6 hours after the start time. [$1.43 \mu\text{l O}_2 \text{l}^{-1} \text{h}^{-1} = 1 \mu\text{g O}_2 \text{dm}^{-3} \text{h}^{-1}$].

(Haynes, Barton, & Pilling, 1993), so the present feature seems anomalous in that it arises upstream rather than downstream of Cabo Bojador. It has been observed though, that in the California Current system, the position of filaments may be quite variable (Huyer, Kosro, Fleischbein, Ramp, Stanton, Washburn, Chavez, Cowles, Pierce, & Smith, 1991; Ramp, Jessen, Brink, Niiler, Daggett, & Best, 1991).

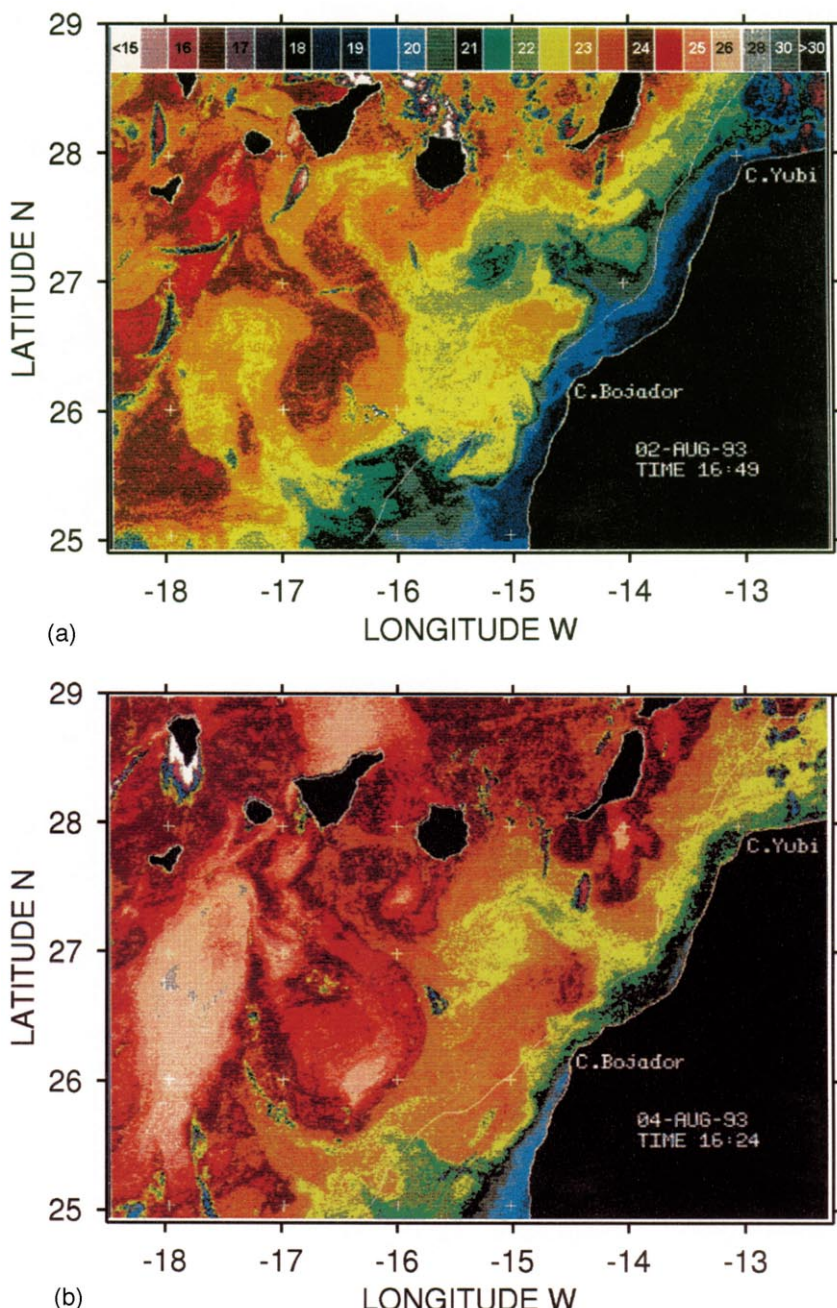


Fig. 11. Series of AVHRR SST images on (a) 2 August (b) 4 August (c) 10 August (d) 18 August (e) 29 August 1993 and (f) wind observed on board *Hespérides* during the period.

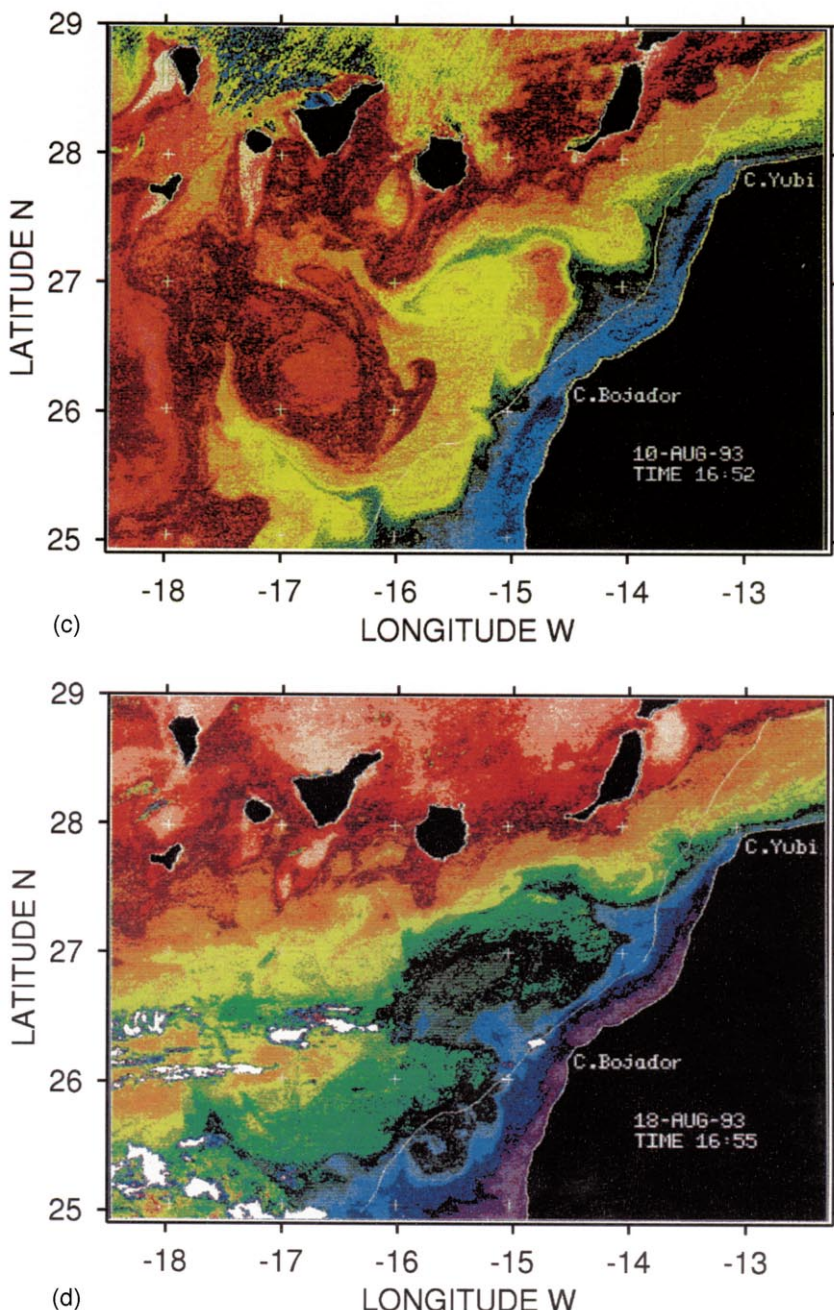


Fig. 11. Continued.

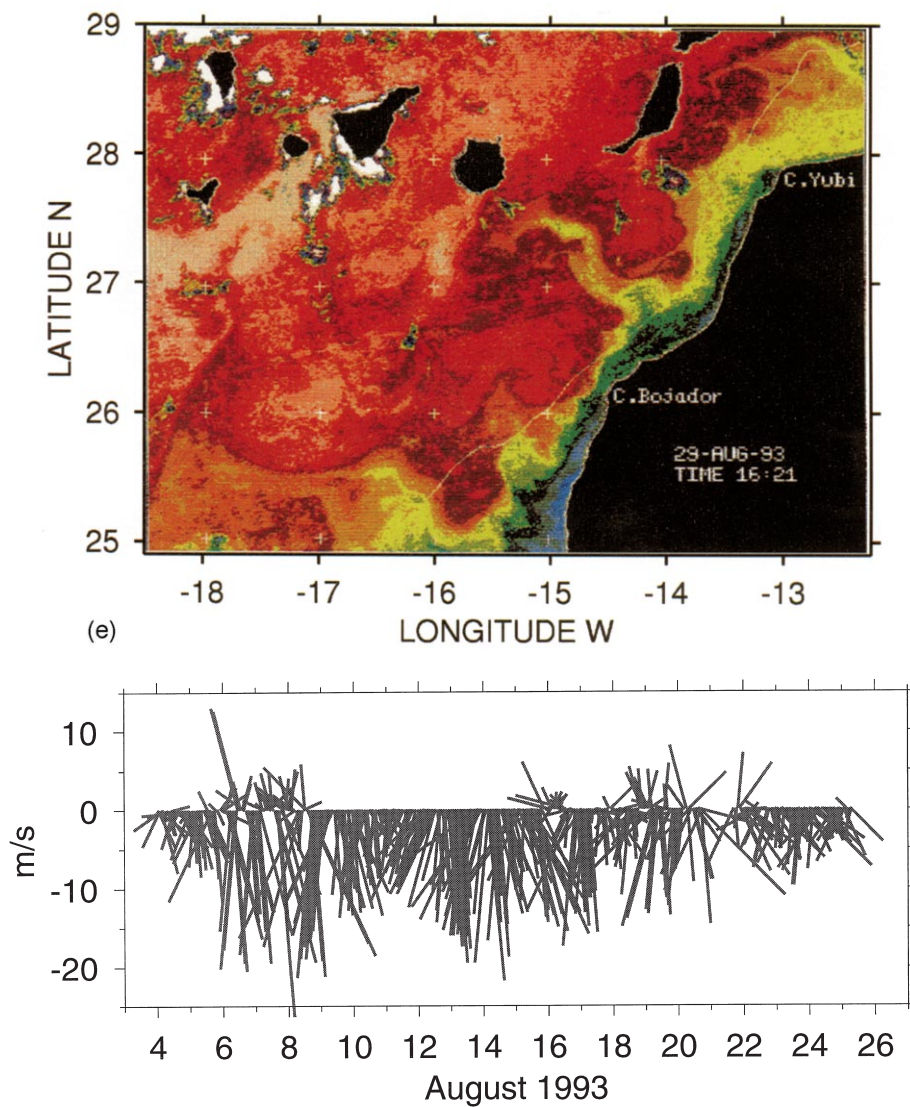


Fig. 11. Continued.

Throughout the image sequence a second filament could be seen extending northwestwards from the shelf about 200 km further south. The offshore limit of the coolest waters in both filaments was at about 150 km from the coast. In several images weakly defined streamers of slightly cooler water extended almost twice as far, but they were probably not directly connected to the filaments.

With the help of the remote sensing imagery, a filament sampling grid was laid out with a standard station spacing of 20 km and closer spacing (of 10, 5 and in

some cases 2 km) in areas of interest like the frontal boundaries. Horizontal distributions reveal that the subsurface structure related to the surface features seen in the SST imagery in a way that changed with increasing depth. At 25 m the temperature distribution (Fig. 12a) retained the form of the filament extending offshore as a well defined tongue of temperatures between 18.5 and 20°C and curving cyclonically towards the south at its offshore limit. The pattern of salinity (Fig. 12b), however, showed only a weak semblance to the near-surface temperature signal and was relatively homogeneous across the area. Highest salinities coincided with higher temperatures in the southwestern offshore waters. The current field measured by shipborne ADCP, overlaid on the 25 m density distribution (Fig. 12c), showed strong structure in relation to the filament. The main feature seen is the large cyclonic eddy around which the filament is entrained. In the near-surface layer (16–25 m) flow paralleled the upwelling front and filament structure. Southward flow entering the area over the continental slope in the northeast, turned sharply offshore around the eddy, and eventually returned shoreward. On approaching the slope some of the flow turned southward to continue along the shelf edge whereas the rest re-circulated about the eddy. Nitrate distributions (Fig. 12d) were sampled only at every second

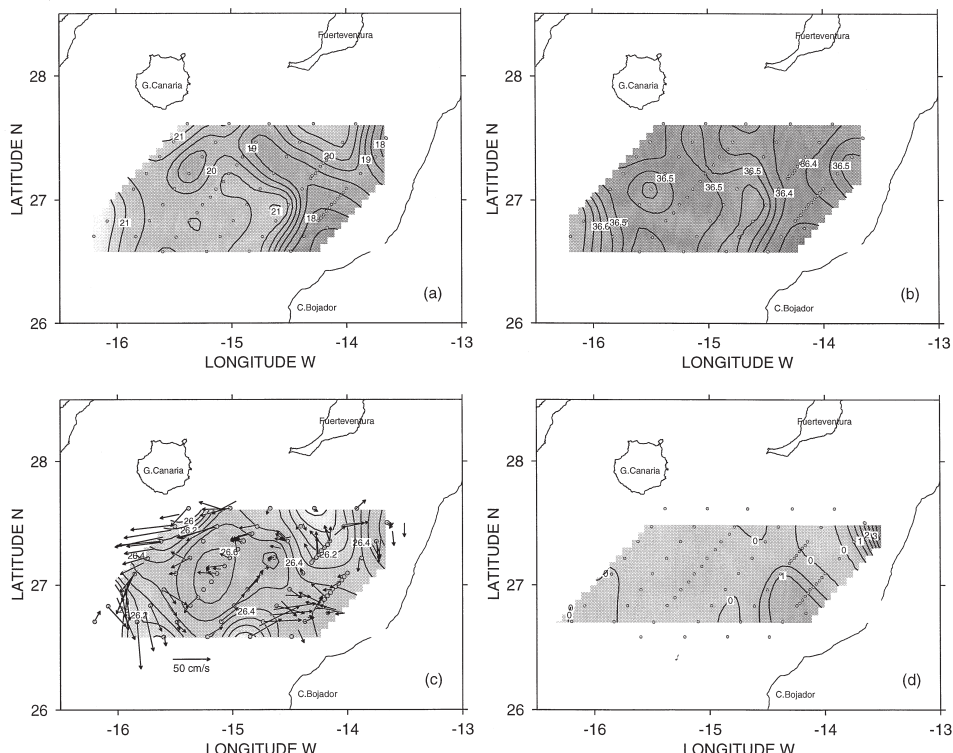
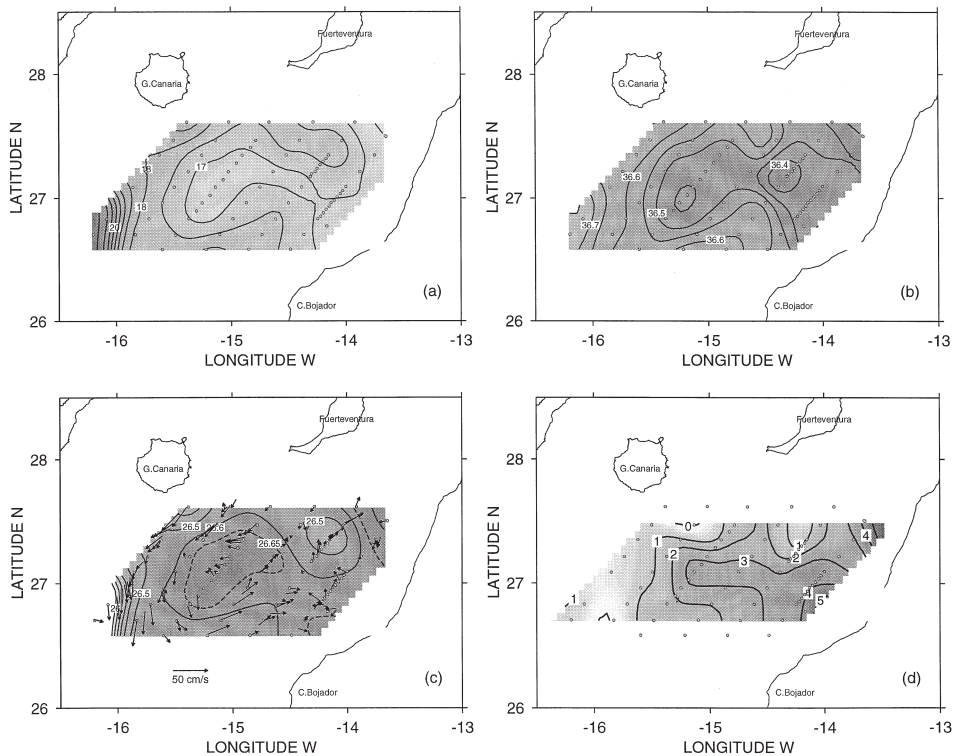


Fig. 12. Maps at 25 m of (a) temperature, (b) salinity, (c) density anomaly and ADCP velocity vectors and (d) nitrate in August 1993.

station but show maximum concentrations in the near surface layer near the African coast. Higher values extended only a short distance offshore in the filament. In offshore waters values were almost zero everywhere.

The distributions at 75 m no longer showed the filament of colder water, but rather a generalised cool area in the centre of the eddy, resulting from the general doming of iso-surfaces in its centre, connected to the near-shore waters affected by upwelling (Fig. 13a). At this sub-thermocline level, salinity and density (Fig. 13b and c) showed strong similarity to temperature. The structure of the currents was similar to that at shallower levels, though flows were generally weaker. At 70 m the nitrate was high over the continental shelf in the areas of coolest near-surface waters (and strongest upwelling), but at this level higher values were also found offshore in the centre of the sample area (Fig. 13d). The cause of the higher nutrient values seemed not to be advection in the filament but more probably upwelling or doming in the centre of the cyclonic eddy.

The map of chlorophyll integrated over the upper 200 m layer (Fig. 14a) also shows highest values near the African coast inside the temperature front marking the offshore edge of the upwelling zone, and a tongue of higher chlorophyll is observed extending northwestwards along the path of the filament. Values generally



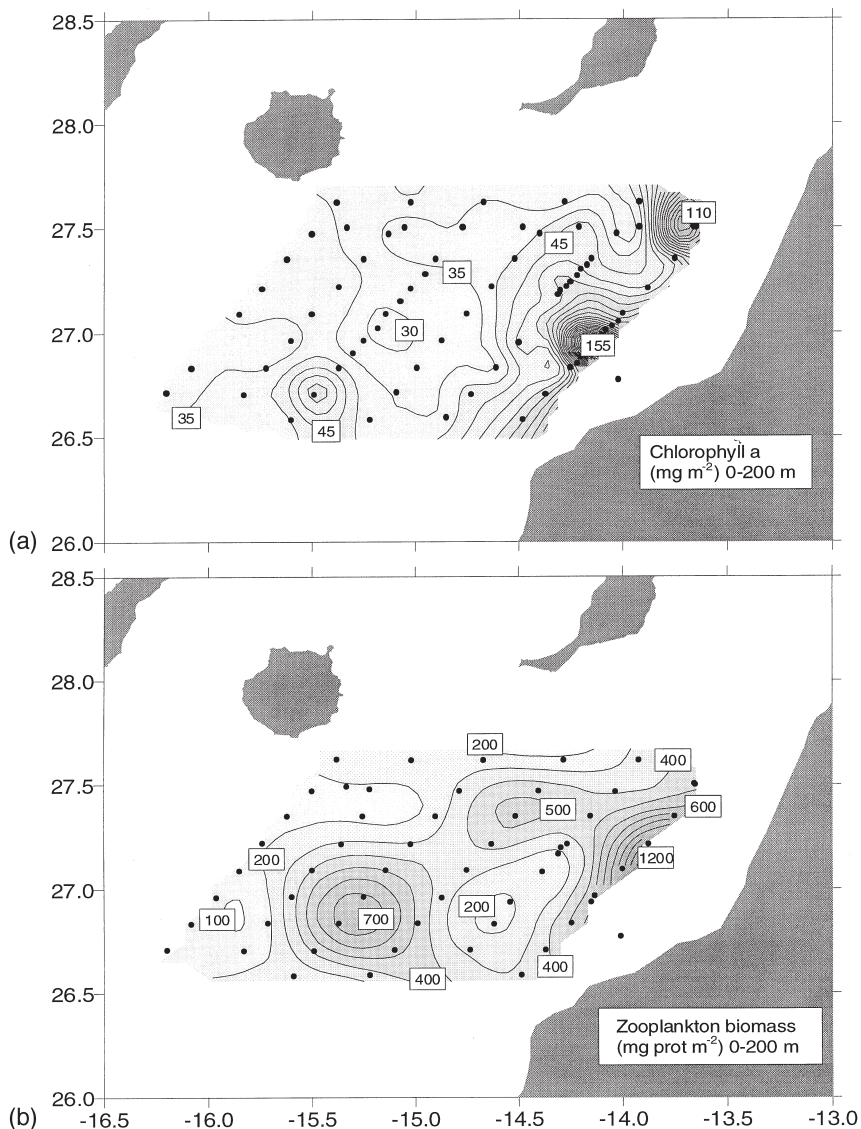


Fig. 14. Maps of (a) chlorophyll, (b) zooplankton biomass, and (c) larval concentration ($/10 \text{ m}^2$) integrated over the upper 200 m.

decreased along the filament and were low in the offshore part of the eddy, but a localised maximum was located in the return flow in its southern part. This coincided with an area of anomalously low salinity at the depth of the pycnocline at 50 m (not shown). The lowest chlorophyll values were observed in the centre of the cyclonic eddy. This distribution might have resulted partly from zooplankton grazing, since the maxima of total zooplankton biomass tend to coincide with chlorophyll minima

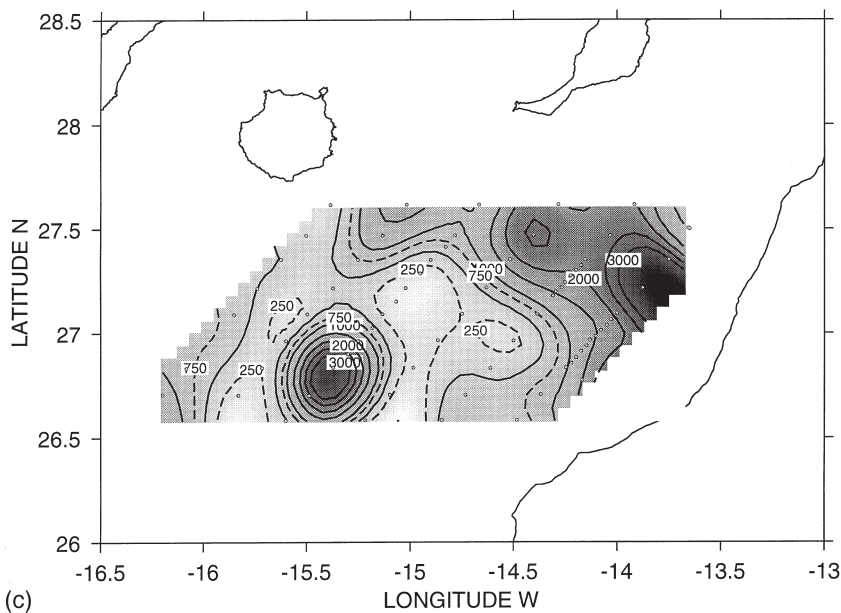


Fig. 14. Continued.

(Fig. 14b). However, it could also be that in the eddy centre phytoplankton had not had sufficient time for significant growth.

The distribution of fish larvae (Rodríguez, 1996) showed a strong dependence on the physical situation (Fig. 14c) as might be expected for organisms that are mainly passive drifters. The larval distributions showed high concentrations occurring on the shelf and reducing along the filament, but with an isolated maximum on the southern flank of the eddy coincident with high zooplankton standing crop. The largest component of the larvae was the sardine *Sardina pilchardus* (28% of all larvae), which are known to be spawned on the continental shelf. These sardine larvae were found only on the shelf and in the filament, including the isolated nucleus indicated by the chlorophyll maximum. In contrast, some oceanic larvae were absent from both the filament and shelf waters. Other neritic species were found only on the shelf and extending a short distance along filament. The higher larval concentrations observed to the north of the filament reflect distributions of anchovy, spawned well to the north off Morocco and spread southwards by the general alongshore flow.

A section parallel to the coast some 20 km offshore of the shelf edge reveals the structure of the filament (Fig. 15). Its width from the surface thermosalinograph trace was about 28 km. Minimum temperature in the filament was 2.5°C lower than in surrounding waters. Surface salinity increased by about 0.2 from north to south across the filament. Near-surface isotherms and isopycnals sloped steeply up from about 50 m depth on either side of the structure, while subsurface isohalines were strongly perturbed down to 150 m. The isosurface slopes weakened at greater depths, becoming undetectable below about 250 m. The deep chlorophyll maximum present

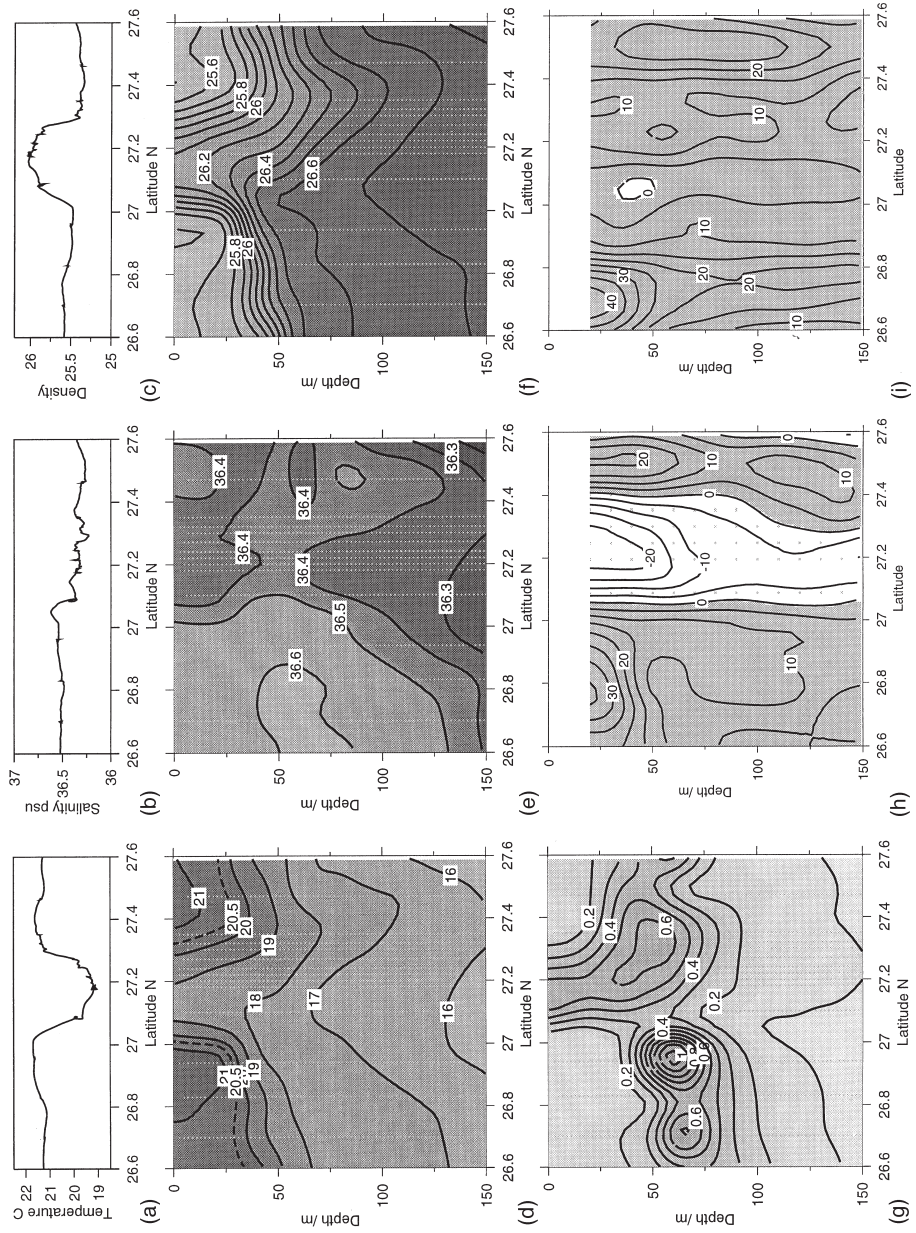


Fig. 15. Section across the filament 30 km beyond the shelf edge showing (a) surface temperature, (b) surface salinity, (c) surface density anomaly, (d) temperature, (e) salinity, (f) density anomaly, (g) fluorescence chlorophyll, (h) offshore and (i) onshore velocity components in August 1993. Velocity component are rotated so that positive onshore (alongshore) components are normal (parallel) to the section towards 134 (44) degrees.

at the base of the pycnocline was interrupted by the filament where maximum chlorophyll values occurred at the sea surface. The ADCP currents showed a core of offshore (normal to the section) flow up to 0.25 m s^{-1} associated with the northern edge of the cold filament and extending to over 200 m depth. To the south of the filament, the layers above 50 m were flowing shoreward with speeds over 0.35 m s^{-1} but at greater depths the flow weakened to about 10 m s^{-1} . To the north of the filament onshore flow with a near-surface maximum of 0.20 m s^{-1} extended down to 175 m depth. Almost everywhere the alongshore component of flow (parallel to the sections) was poleward with strongest flow of 0.45 m s^{-1} occurring near-surface at the southern end of the transect and a weaker maximum at its northern end. The lack of any clear indication of convergence or divergence in the cross-filament flow in association with the high surface chlorophyll and low temperature suggests that they are the results of advection along the filament rather than local vertical processes.

The filament signal weakened with distance offshore and was barely detectable in the furthest offshore CTD sections. A transect at about 150 km offshore with 10 km station spacing (Fig. 16) failed to detect the subsurface structure of the filament. It was still evident in the surface thermosalinograph trace as an 8 km wide temperature minimum (1°C cooler than surrounding waters) and salinity step of 0.2 centred near 27.38°N . A wider, weak near-surface temperature minimum of $<20.5^\circ\text{C}$ near 27°N seen in the temperature section represents a weak continuation of the filament being entrained around the eddy as seen in the satellite image of Fig. 11c. Below 50 m depth all variables indicated a smoothly domed structure, indicative of the cyclonic circulation around the eddy. The general deep chlorophyll maximum was strongest beneath the two surface temperature minima in the filament. The separation into two maxima reveals entrainment of the deep chlorophyll maximum around the cyclonic eddy. This is consistent with the flow field, which is offshore north of 27°N and onshore to the south. Everywhere along this section the alongshore component of flow was equatorward with a minimum near 27°N close to the eddy centre. Volume transport, estimated from the ADCP observations, was about $10^6 \text{ m}^3 \text{ s}^{-1}$ in the filament where it crossed the nearer-to-shore transect. Further offshore, the broader flow around the eddy, including the entrained filament, had more than twice this transport (Navarro-Pérez, 1996).

Chlorophyll generated in the African upwelling system may be spread into the eastern Canary region or transported by filaments some hundreds of kilometres offshore, extending out as far as south of Gran Canaria (Hernández-Guerra, Arístegui, Cantón, & Nykjaer, 1993; Arístegui, Tett, Hernández-Guerra, Basterretxea, Montero, Wild, Sangrá, Hernández-León, Cantón, García Braun, Pacheco, & Barton, 1997). Previous observations on the offshore boundaries of filaments at the southeastern Canaries (Montero, 1993; Basterretxea, 1994; Arístegui, Tett, Hernández-Guerra, Basterretxea, Montero, Wild, Sangrá, Hernández-León, Cantón, García Braun, Pacheco, & Barton, 1997) coincided in that filaments were always transporting higher concentrations of chlorophyll to open ocean waters. However, the phytoplanktonic community composition is not always the same. In the October 1991 cruise, the filament was transporting relatively large amounts of cyanobacteria. In March 1991 and August 1993 the trend was the opposite: the upwelled waters contained lower

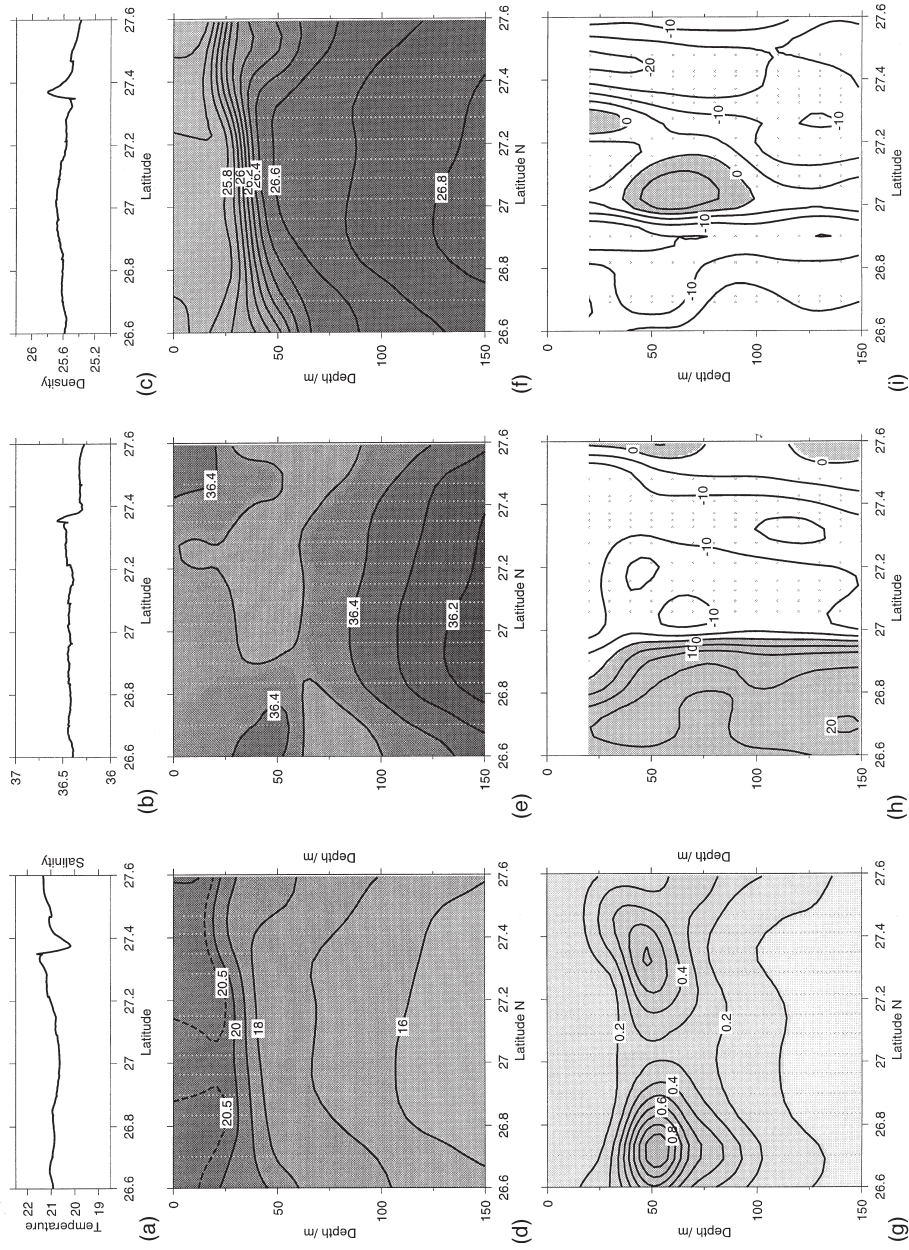


Fig. 16. Section 150 km offshore as Fig. 15.

abundances of cyanobacteria but relatively higher numbers of eukaryotic cells (Ballesteros, 1994; Barton, 1994b). This may indicate a different source and age of the offshore advected water. It is possible that diatoms, when strongly flourishing in the upwelling on the shelf, sink as they are transported offshore in the filament, or are grazed, leaving some new or recycled nutrients to stimulate the growth of small-celled phytoplankton entrained into the filament from the ocean water.

The role of upwelling filaments in transporting nutrients into the Canary region is not as evident as with chlorophyll. Whilst little information is available (e.g. Bassterretea, 1994) indicates that dissolved inorganic nutrients like nitrate are already exhausted in surface waters of upwelling filaments arriving to the south of Gran Canaria, as seen in Fig. 12d. Nevertheless, deep waters upwelling in the core of cyclonic features associated with filaments may be important local sources of nutrients in the offshore regions (e.g. Hayward, & Mantyla, 1990), as seen in the August cruise (Fig. 13d). It is however plausible that under certain situations a net horizontal transport of nutrient-rich coastal upwelled waters could be produced, enhancing productivity in open ocean waters. Intense newly formed upwelling filaments may transport nutrient-enriched waters out into the open ocean before the nutrients become exhausted by phytoplankton (Jones, Mooers, Rienecker, Stanton, & Washburn, 1991). Conversely, if the advection of upwelled water is slower, there will be almost complete utilization of the nutrients by phytoplankton close to the African coast. In either situation both particulate and dissolved organic matter are exported into the eastern Canary region enhancing microbial respiration (Montero, 1993).

In all instances the transport of organic material seems to be a more important process than the dissolved nutrient transport. The representation of nutrients, chlorophyll concentrations and ETS activity along a vertical section extending from upwelled waters to open ocean waters during the August cruise shows that gradients in chlorophyll and ETS activity extend farther offshore than nutrients (Fig. 17). Chlorophyll and ETS activity maxima coincide at stations closest to the African coast, indicating that in the upwelling near to shore respiration is mainly by phytoplankton. However further offshore, the maximum in ETS activity occurs at a shallower level than the DCM suggesting that here the activity is more likely to be the result of bacterial respiration utilising the dissolved organic material produced inshore by photosynthesis in the upwelled water and then advected offshore by the filament. In this long section, south of the islands chain, two cyclonic eddies and one anticyclonic eddy are evident. One of the cyclonic features, located in otherwise oligotrophic waters at distance of 120 km (south of the island of La Palma), showed a significant upward displacement of isopleths. This doming, especially visible in the nitrate section, was apparently producing an increase in chlorophyll concentration and respiratory activity similar to the situation in the coastal upwelling zone.

4.2. Island eddies

Eddies generated by islands in the Canary region were first identified by remote sensing (Hernández-Guerra, Arístegui, Cantón, & Nykjaer, 1993) and their structures later observed by AXBTs and CTD surveys (Arístegui, Sangrá, Hernández-León,

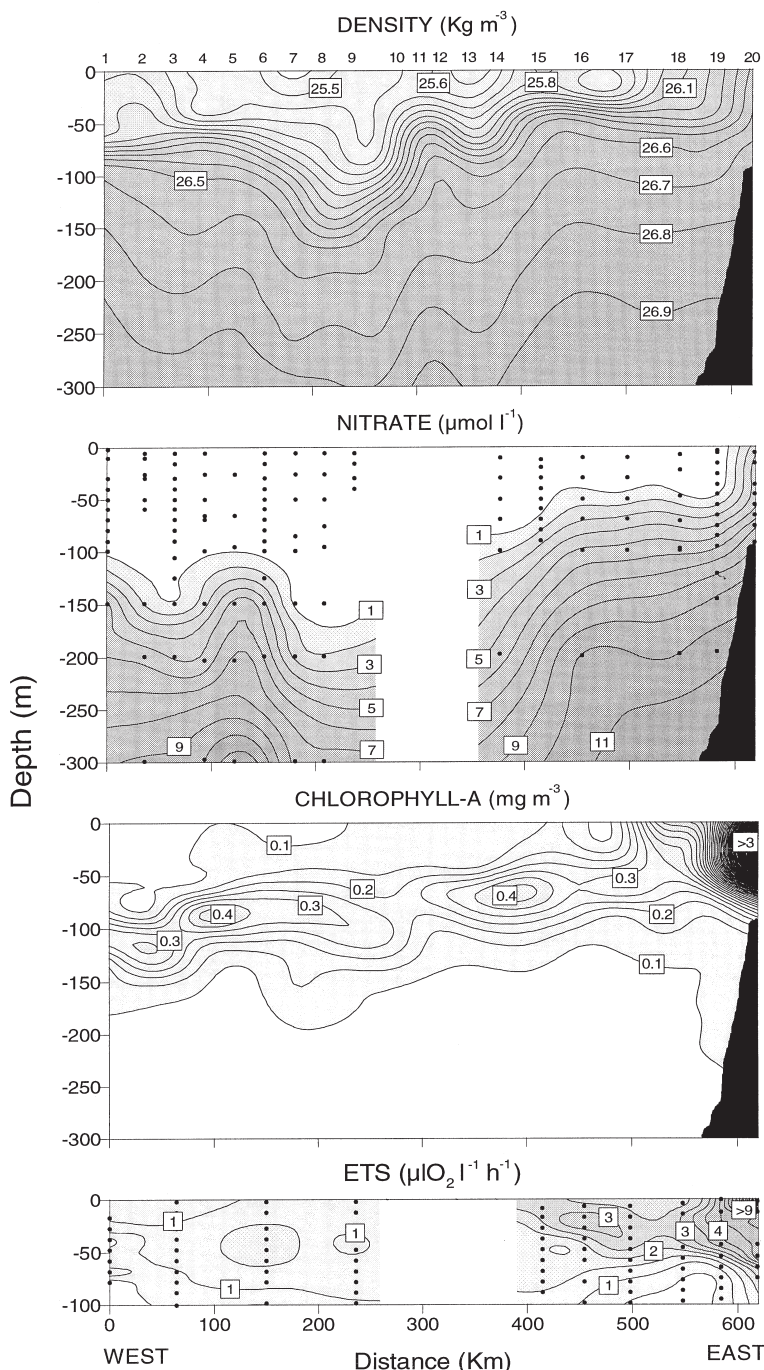


Fig. 17. Long section (H in Fig. 2) south of the archipelago showing density anomaly, nitrate, chlorophyll and ETS activity in microplankton in August 1993. Sampling was interrupted in mid-section by strong winds. [$1.43 \mu\text{l O}_2 \text{l}^{-1} \text{h}^{-1} = 1 \mu\text{g O}_2 \text{dm}^{-3} \text{h}^{-1}$].

Cantón, Hernández-Guerra, & Kerling, 1994). Eddies downstream of Gran Canaria have been studied thoroughly by both satellite and in situ observations (Barton, 1994a; Arístegui, Tett, Hernández-Guerra, Basterretxea, Montero, Wild, Sangrá, Hernández-León, Cantón, García Braun, Pacheco, & Barton, 1997); satellite observations indicate that eddies are also produced downstream of the other islands like Tenerife, Gomera or La Palma. The long section south of the Archipelago depicted in Fig. 17 illustrates the presence of cyclonic and anticyclonic structures in the vicinity of several of the islands. Typically, a cold-core cyclonic eddy is found to the southwest of Gran Canaria. On certain occasions a second warm-core anticyclonic eddy has been also observed to the southeast giving rise to a structure like a von Karman vortex street. However, the extension of the Cape Bojador upwelling filament towards the south of Gran Canaria presumably inhibits the development of the anti-cyclonic feature in most situations. Another factor which favours cyclogenesis is potential vorticity conservation as the flow encounters deeper waters on leaving the channels between the islands. Eddies have been observed even during the lowest wind intensity periods. This led Arístegui, Sangrá, Hernández-León, Cantón, Hernández-Guerra, & Kerling (1994) to suggest that they are produced as result of the flow past the island, as modelled by Sangrá (1995).

In October 1991 during and after a very low wind period there was clear evidence of a cyclonic eddy to the southwest of the island (Fig. 18), which could be seen at subsurface levels to at least 200 m depth. The surface expression of this cold core eddy was barely apparent because of the strong near surface stratification; isopycnal doming was most pronounced at around 150 m. Nevertheless, the intensity of the eddy (calculated from the ratio between the elevation and eddy radius on the 16°C isotherm) was of the same magnitude as other eddies found during stronger wind periods. Evidence of chlorophyll enhancement around the periphery of the eddy (Fig. 19) was compatible with active pumping of sub thermocline water into the euphotic zone and the uplifting of the DCM to better illuminated depths. Lower chlorophyll values in the eddy centre may reflect the direct effect of strong upwelling of low chlorophyll, nutrient-rich waters coupled with a relatively slow rate of phytoplankton growth.

In March 1991 an anticyclonic and two cyclonic eddies forming a vortex street were studied (Fig. 18). A vertical section crossing one cyclonic and the anticyclonic eddy from west to east shows higher chlorophyll near the upper dome of the cyclone and in the eastern waters of African origin (Fig. 19). Although the March and October cruises were limited in the extent of sampling and areal coverage, during both there was evidence of the influence of water originating in the African coastal upwelling reaching almost to the island of Gran Canaria. A strong boundary was seen to the south and southeast of the island, clearly separating oceanic waters from those transported offshore in the filament from the coastal upwelling. Apart from their contrasting T-S properties, these waters were clearly differentiated by their biological and chemical properties. In particular the coastal upwelled waters always contained higher concentrations of chlorophyll.

In August 1993, an intense cyclonic eddy was once again observed to the southwest of Gran Canaria in the satellite imagery and in situ observations (Figs. 20 and

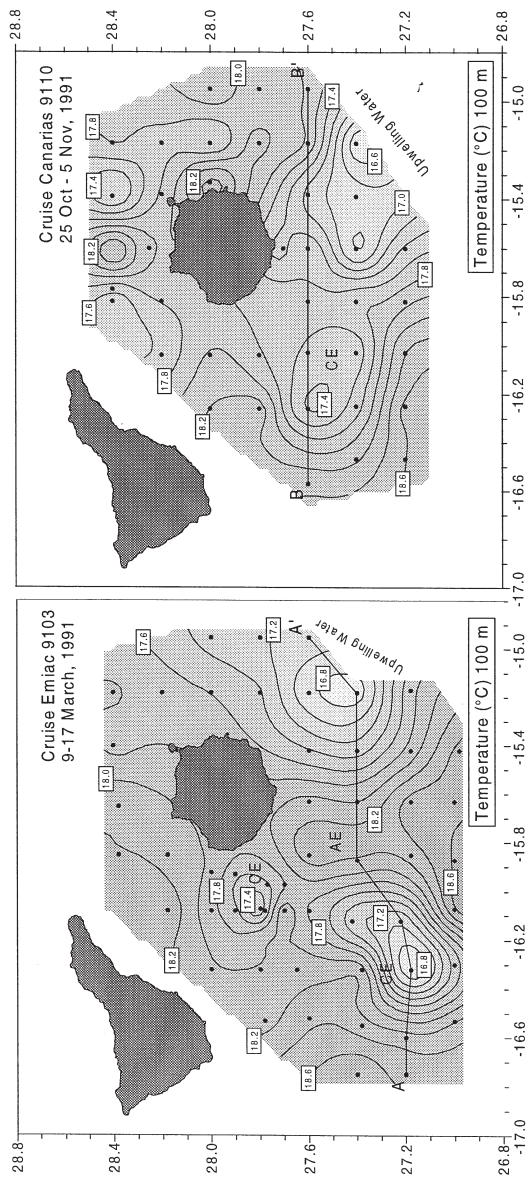


Fig. 18. Maps of temperature at 100 m depth during eddy surveys in March and October 1991 (Box E in Fig. 2).

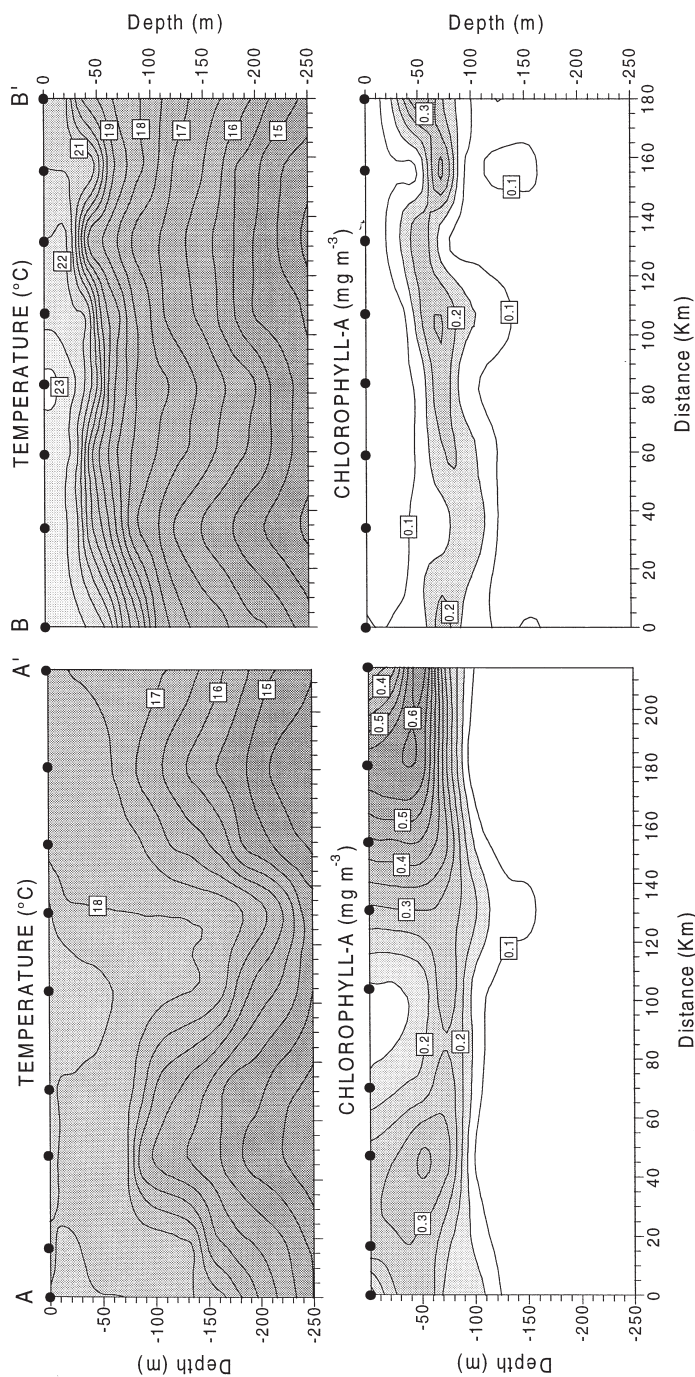


Fig. 19. Sections of temperature and chlorophyll across the transects AA' and BB' marked in Fig. 19.

11c). It was located in a similar position to those sampled during earlier cruises and observed on other occasions by remote sensing. Two eddy surveys (Fig. 21) were made during the *Hespérides* cruise with a separation of three days, during which time the eddy drifted southwards at a speed of about 0.15 m s^{-1} . An Argos drifter dropped close to the estimated centre after the first survey drifted with and around the cyclonic eddy (Fig. 22). Azimuthal velocities with respect to the centre (position linearly interpolated between surveys) were around 0.5 m s^{-1} . The drifter made one almost complete circuit in three days, but also moved out from the centre at an average speed between 0.15 and 0.2 m s^{-1} after the first day of apparent oscillation. Poor knowledge of the precise position of the eddy centre makes the velocity estimates subject to uncertainty at the start. If the later, steadier velocity represents a true radial motion, then it implies a high upwelling speed in the eddy centre. If the outward velocity was occurring over an upper layer depth of 50 m at a radius of 25 km , this implies that the upward velocity was more than 50 m d^{-1} . Since it was possible that there was imperfect coupling between drifter and water column and other factors such as changing background shear (Shapiro, Barton, & Meschanov, 1997) may have influenced the drifter trajectory, the upwelling estimate must be taken as an upper limit.

Despite these reservations, sections across the eddy during the two surveys show

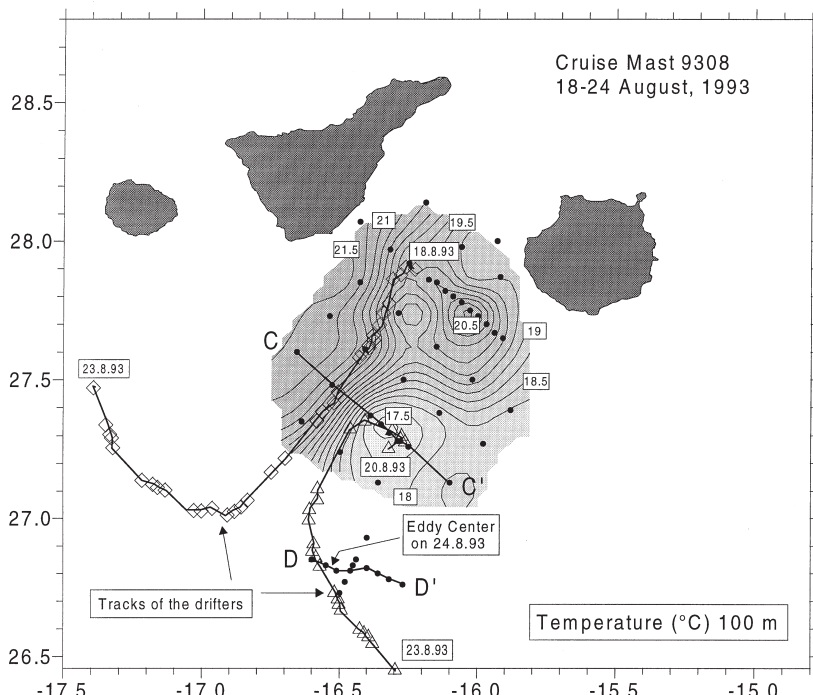


Fig. 20. Maps of temperature at 100 m during August 1993 with drifter tracks superimposed. Open triangles and diamonds indicate drifter Argos fixes. Start and end dates are shown.

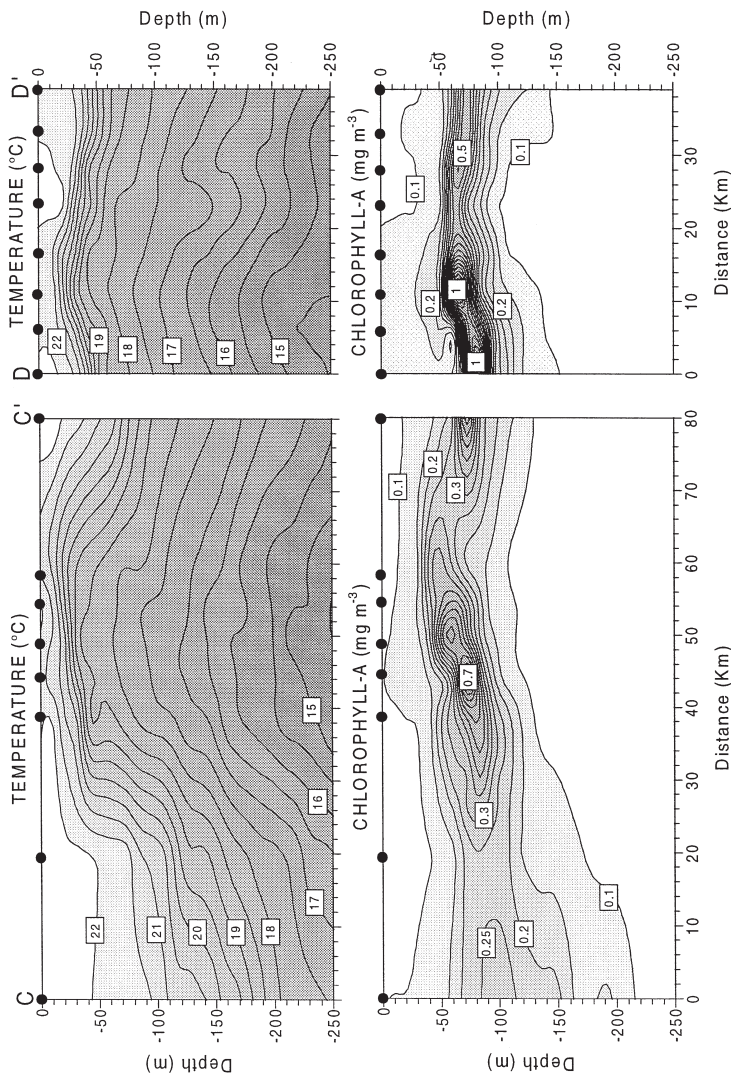


Fig. 21. Sections of temperature and chlorophyll across the transects CC' and DD' marked in Fig. 21.

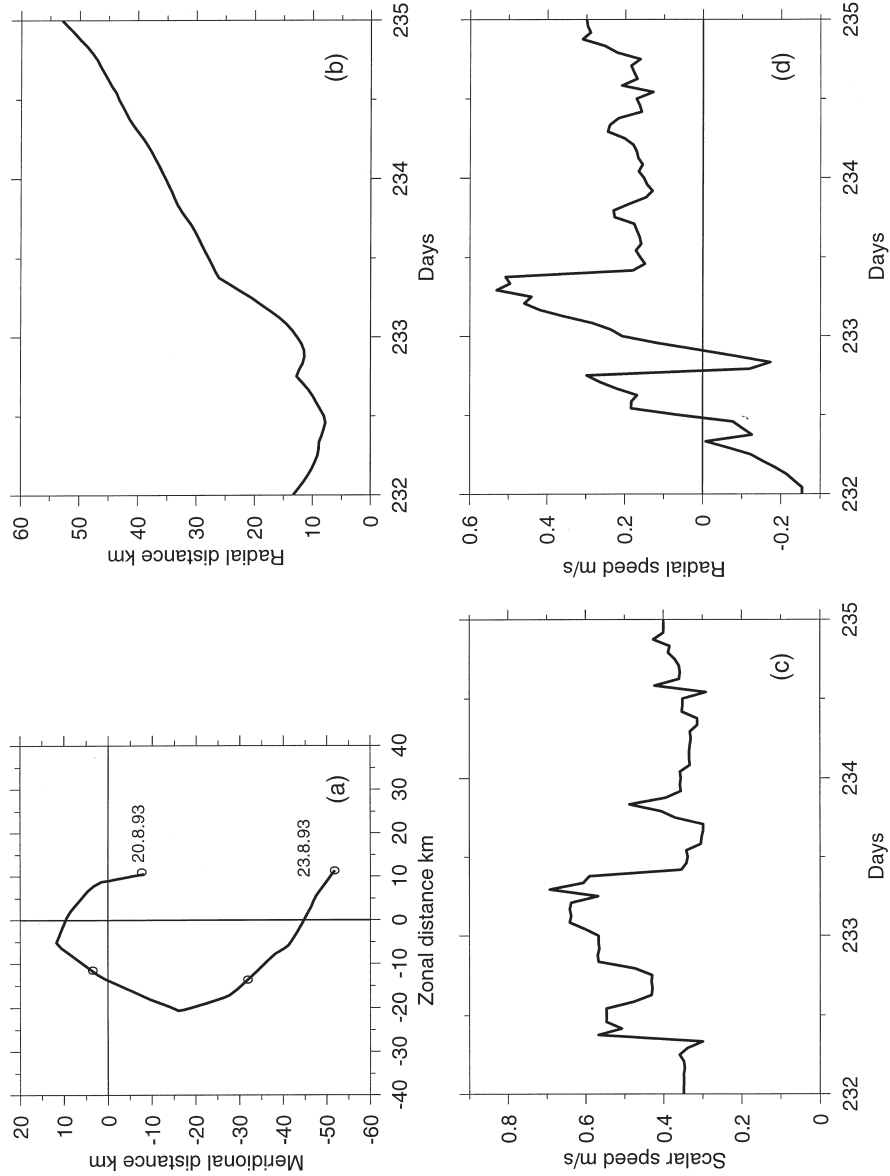


Fig. 22. (a) Drifter trajectory relative to centre of cold-core eddy. Positions interpolated to midnight are marked by a circle (b) Separation distance of drifter from eddy centre estimated by interpolation between positions during two surveys (c) Scalar drifter speed along trajectory (d) rate of increase of separation from estimated eddy centre. Year Day 232 is 20 August 1993.

large vertical excursions of the isosurfaces of up to 150 m in the centre (Fig. 21). Although the later survey was less extensive, and did not show the structure so clearly, the isotherms were just as shallow in the centre as initially. A marked increase in the intensity of the DCM at the top of the eddy dome was evident between the two eddy surveys. This contrasts with the observed chlorophyll enhancements at the periphery of eddies closer to the island (e.g. in the March cruise). Several mechanisms have been proposed to explain chlorophyll distributions in island eddies (Aristegui, Tett, Hernández-Guerra, Basterretxea, Montero, Wild, Sangrá, Hernández-León, Cantón, García Braun, Pacheco, & Barton, 1997). In particular, eddies closer to islands are thought to be at earlier developmental stages than those that have already spun off. The former would have higher upward transport of deep nutrient-rich water in their cores and hence a low chlorophyll content, whereas in older eddies there would have been more time for the growth of phytoplankton to have become apparent.

A second drifter deployed in the channel between Gran Canaria and Tenerife moved rapidly southwestwards and then turned anticyclonically with a radius of about 50 km back towards La Gomera and Tenerife (Fig. 20). Although no detailed survey was carried out at the time, the earlier long section across the south of the islands clearly shows a strong downbowing of isopycnals and other surfaces associated with an anticyclonic eddy to the south of Tenerife (Fig. 17). Whether this is a recurring feature like the cyclonic eddies is not known.

4.3. Island lee

Warm lee regions occur downwind of the elevated topography of many of the Canary Islands (Fig. 11). During the August 1993 cruise, sampling was carried out across the warm lee region southwest of Gran Canaria from the exposed waters to the east almost to those on the west. An impression of the lee is given by Fig. 23 which shows wind vectors and the associated density section on 8–9 August when the research vessel was sheltering from particularly strong Trades. Stations were spaced at about 2 km along the sampling line, which was oriented perpendicular to the predominant Trade wind direction. Wind conditions at the time prevented working in the fully exposed ocean, and so one additional station made several days later is included to show conditions further southeast. At the anticyclonic wind shear boundary wind dropped from $> 15 \text{ m s}^{-1}$ to virtually zero over three stations. The shear line was visibly evident from the abrupt contrast in sea state, which changed over a short distance from rough breakers in the exposed area to calm in the lee.

The effect of the wind structure is seen in the vertical distributions across the boundary (Fig. 23). In the density section a strong downward slope from northwest to southeast is seen in all the isopycnals across most of the section, but at the eastern end they slope upwards again to shallow levels. In the centre of the lee region a pool of low density surface water corresponds to the ‘warm wake’ evident in satellite images. Here daytime heating in the absence of strong wind mixing leads to the formation of a thin warm stratified surface layer. In the exposed regions the effect of surface heating is masked by the strong wind-induced mixing to produce a uniform

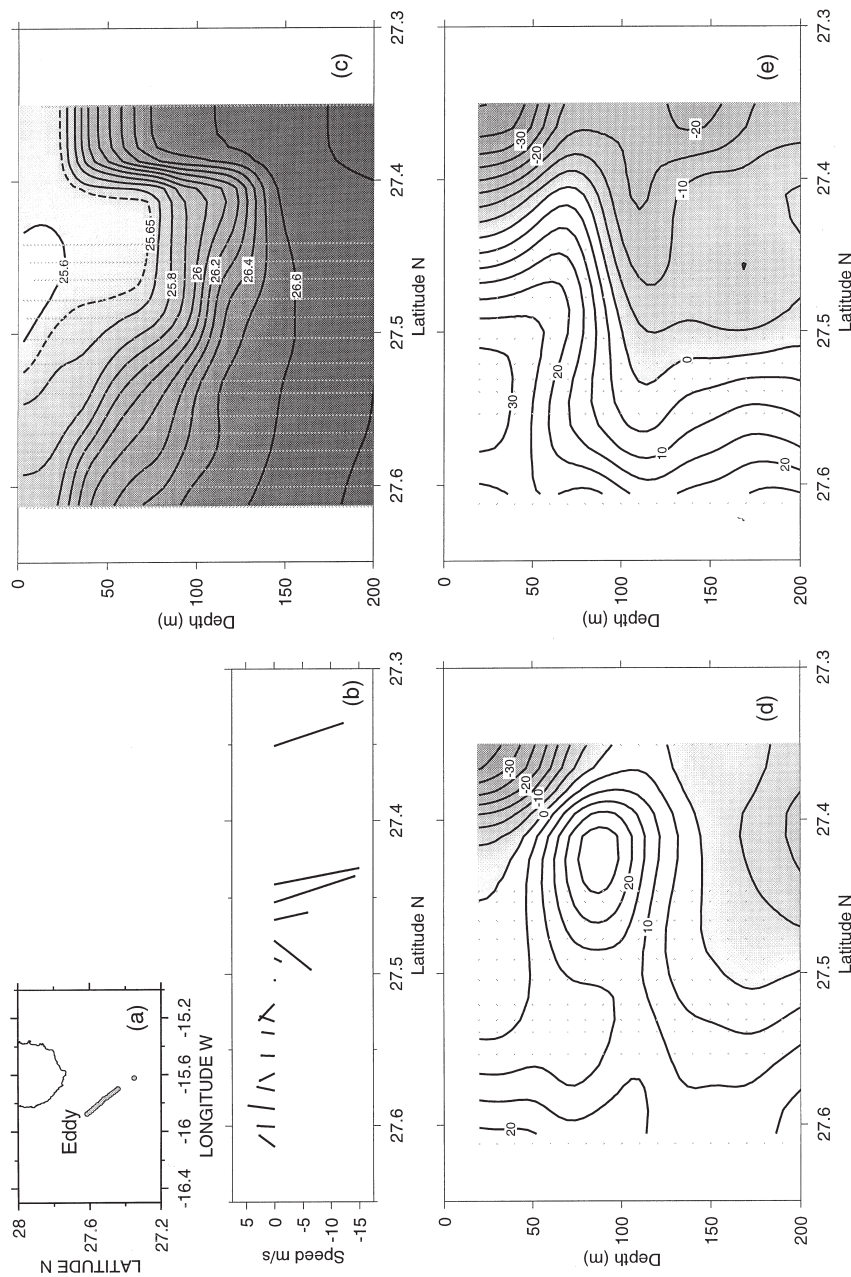


Fig. 23. Section across the lee region of Gran Canaria in August 1993 (a) station positions (b) wind vectors rotated into direction of principal axes of winds during the cruise (up the page represents direction towards 64.5 degrees) (c) vertical section of density anomaly (d) along-section (positive to southeast) and (e) across-section (positive towards northeast) components of ADCP velocity.

surface layer. The pycnocline across the lee region is elevated at the cyclonic wind shear end and depressed at the anticyclonic end. These distortions of the pycnocline could well be the result of Ekman pumping, which will cause vertical velocities of the same magnitude as in the coastal upwelling. The observed wind speeds of around 15 m s^{-1} would produce vertical motion of $5\text{--}10 \text{ m d}^{-1}$ over a typical Rossby radius of about 15 km.

The ADCP velocity components, rotated parallel and perpendicular to the section (Fig. 23d and e), show strong shear and convergence of currents across the wind shear zone. A component of flow towards the boundary from the southeast is indicated at the easternmost stations, where significant southwestward flow is also seen. In the lee region itself flow above 100 m is mainly northeastward, normal to the line, with small component along the section. Since the easternmost station is on the outer edge of the filament and large cyclonic eddy system the flow in that location is probably more representative of the filament than of any particular dynamics associated with the lee region. The importance of possibly transient effects such as the maximum of cross boundary flow at 100 m (amplified in the interpolation between the two most eastern ADCP profiles) can only be determined with more extended sampling.

Any vertical velocities would be maximal on the boundary between the well-mixed surface waters exposed to the wind and the sheltered waters, subject to strong diurnal surface heating, in the lee. Strong wind events provide upward and downward impulses to the pycnocline on either side of the island. The resultant perturbations have a downstream scale on the order of an island diameter, and so represent a possible mechanism for the production of the eddies observed in the wake of the islands, additional to the conventional one of eddy shedding by flow past an obstacle. Indeed, a cyclonic eddy was observed in the satellite image of 10 August (Fig. 11c) one and a half days after the in situ sampling, centred just the western end of the section shown in Fig. 23. This was the same eddy that was sampled later in the cruise after having drifted to the southwest. The Ekman pumping velocities estimated at the boundaries of the lee are smaller than the eddy upwelling rate estimated from the drifter deployed in the cyclonic eddy, which may indicate over-estimation of the latter. The relative contributions of wind-induced Ekman pumping and island eddy shedding to production of both cyclonic and anticyclonic eddies require further investigation, but these results show that the two phenomena are linked.

5. Discussion

The interaction between the northwest African coastal upwelling and offshore waters is seen to be governed by mesoscale activity in the form of filaments, eddies and island wakes. A major focus of this study, the filament, was sampled at the time of strongest wind forcing when the strongest upwelling signal was present. In the cruises made at other times of year, the offshore boundary of the filament was present in much the same location south east of Gran Canaria. Although remote sensing imagery has shown its presence at various times of year (Hernández-Guerra,

Arístegui, Cantón, & Nykjaer, 1993; Van Camp, Nykjaer, Mittelstaedt, & Schlittenhardt, 1991) there is still no clear idea of its persistence or evolution over the yearly cycle and no information is available on its subsurface structure. The work reported here provides many details of its physical structure and extent, the related velocity field, and its biology and chemistry. These allow estimates of transports and fluxes to be made, and their importance to coastal—open ocean exchanges to be assessed.

Filament structures have been documented in the coastal upwelling regimes off California (Brink, & Cowles, 1991), Portugal (Haynes, Barton, & Pilling, 1993) and southwestern Africa (Lutjeharms, & Stockton, 1987) during their respective coastal upwelling seasons. Though their occurrence seems ubiquitous, their development has been attributed to a variety of different causes, and investigated in numerous modelling and laboratory rotating tank studies. Strub, Kosro, & Huyer (1991) summarized the principal ideas of filament formation in terms of three simplified conceptual models.

The first model is that of ‘squirts’ or one-way jets, transporting coastally upwelled water into the deep ocean, sometimes terminating in a counter-rotating vortex pair. Frequently occurring patterns of sea surface temperature and pigment fields, denoted as ‘mushroom,’ ‘hammerhead,’ or ‘T’ by Ikeda, & Emery (1984), have been considered to be squirt-like. The idealized squirt is generated by near-shore convergence, caused by local wind relaxation around capes (Huyer, & Kosro, 1987) or blockage of the current by a cape or offshore extending ridge.

The second conceptual model consists of a field of mesoscale eddies imbedded in a slow southward current (Mooers, & Robinson, 1984). Where the eddies draw recently upwelled water away from the coast, they create a surface temperature structure similar to a squirt.

The third conceptual model is based on a continuous, meandering southward jet, which entrains coastally upwelled water near-shore and creates filaments of cold, rich water, extending along the next offshore meander. Closed eddies may be created on either side of the jet by instabilities of the flow, but water in the core of the meandering jet may originate from far upstream, which would not be the case for a squirt and would occur only haphazardly in a mesoscale eddy field.

The filament described here does not correspond neatly with any of the three filament production mechanisms of Strub, Kosro, & Huyer (1991). It seems to be a quasi-permanent feature, which has been noted in satellite images of the region over many years. La Violette (1974) reported Airborne Expendable Bathythermograph observations and early remote sensing of sea surface temperature in the area, which can now be recognised as indicating structure similar to that discussed here. Observations south of Gran Canaria have indicated the influence of an upwelling filament close to the island on several occasions apart from our March and October 1991 cruises (Arístegui, Sangrá, Hernández-León, Cantón, Hernández-Guerra, & Kerling, 1994; Arístegui, Tett, Hernández-Guerra, Basterretxea, Montero, Wild, Sangrá, Hernández-León, Cantón, García Braun, Pacheco, & Barton, 1997). The filament in this location is strongly related to the existence of a, seemingly, permanent cyclonic eddy situated in the trough between Gran Canaria and the African coast. The close relation of the flow field with bottom topography indicates that the origin of this eddy is

most likely vortex stretching of the flow exiting the shallower (< 1500 m) channel between the archipelago and Africa. Whenever upwelling is well developed over the continental shelf, the outer boundary of the cold water and associated alongshore current jet may extend far enough offshore to become entrained around the eddy, so producing the filament. The recurrence of the filament at the same site is indicated by a distinct long term mean temperature minimum extending from north of Cabo Bojador towards Gran Canaria in the average SST image of Fig. 1. With only one realisation of the filament's in situ structure, the variability of the system, which may be significant, remains undetermined. Possible indications of short term variability are the isolated extrema of salinity, chlorophyll and larval density observed on the southern flank of the eddy (Fig. 14). Such features might be produced by intermittent periods of more intense coastal upwelling so that temporal variability at the coast results in spatial variability along the filament.

Another recurrent filament occurs off Cape Ghir some 200 km north of the Canaries. Hagen, Zülicke, & Feistel (1996) have reported that it arises from interaction of the alongshore flow with a local plateau in bottom topography. The filament was formed as one branch of a coastal upwelling jet, the other branch of which continued alongshore through a weak cyclonic meander. The tongue of cold water extended offshore some 200 km between cyclonic and anticyclonic eddies, downstream and upstream, respectively, of the Cape Ghir Plateau. Unlike the present case, there was no indication of a return path to the coast for waters transported offshore in the filament. Transport estimates indicated that upwelling as strong as in the near-shore zone, must occur in the filament itself.

The offshore transport in filaments is often large compared to the Ekman transport. Near to the shelf edge the measured offshore transport in the Cabo Bojador filament was close to $10^6 \text{ m}^3 \text{ s}^{-1}$. Integrating the Ekman transport over the alongshore separation between filaments (200 km) provides a value of $0.4 \times 10^6 \text{ m}^3 \text{ s}^{-1}$, therefore the filament does not simply represent an integration of the wind forcing. The net effect of filament transport may be estimated for the area from the strength, number and temporal occurrence of filaments. The offshore flow in any filament contributes to the net water exchange if water parcels lose their integrity in the offshore region and are not returned intact to the coastal upwelling zone. If the width of the upwelling frontal zone is much less than the offshore extension of the filaments then U_e the net cross-frontal water exchange velocity is given by

$$U_e = n u d t_p$$

where n is the number of filaments per unit distance alongshore, u is the offshore velocity in the filament, d is the filament width and t_p is the relative duration of the filament as a proportion of days per year when the filament is present. Kostianoy, & Zatsepin (1996) estimated, from satellite sea surface temperature images, the number and frequency of occurrence of cold filaments off north west Africa. In their case, with 60 filaments in an alongshore distance of 1000 km, occurring for a duration of 5 days per year, with a typical velocity of 0.4 m s^{-1} and width 30 km (estimated from one filament), they found $U_e = 0.01 \text{ m s}^{-1}$ within a 50% uncertainty. The equivalent horizontal exchange coefficient is given by $K = U_e D = 500 \text{ m}^2 \text{ s}^{-1}$, where

D is the frontal width. They also made estimates of these values for the southwest African region, with similar results.

In the present case, filaments occur at separations of about 200 km to both south and north (off Cape Ghir) of the one studied. The width of this filament is about 25 km and it persists for most of the year. Taking a typical near-surface offshore velocity as 0.4 m s^{-1} , a value for the net exchange velocity is $U_e = 0.05 \text{ m s}^{-1}$, and $K = 2500 \text{ m}^2 \text{ s}^{-1}$. These derived values would be reduced proportionately if the mean offshore velocity were smaller or the filament duration were less. They are higher than those of Kostianoy, & Zatsepin (1996) principally because of the estimated lifetime of the filament. In their case, the duration seems short compared to filament lifetimes reported for even the strongly seasonal Portugal (Haynes, Barton, & Pilling, 1993) and California Current (Brink, & Cowles, 1991) regions, where durations of months are common. A second important factor which would reduce the present values is the proportion of water which is returned to the coastal zone by recirculation around the eddy with little effective mixing with oceanic waters. Additionally there is little information to indicate the variability of the filament and eddy system in response to changing winds and currents.

The anomalous combination of low salinity and high zooplankton and fish larvae counts along the southern limb of the cyclonic eddy probably reflects variability in forcing. The time taken for a complete circuit of the eddy (diameter 100 km, tangential speed 0.4 m s^{-1}) is about 7 days. This is comparable to the time taken to sample in situ the entire filament station grid, during which time the wind forcing will have varied significantly. The distributions mapped are, therefore, not truly synoptic though the relative persistence of the principal features of the filament and eddy system seen in the AVHRR images indicates that there had been no gross change in the situation. It is clear, however, that conditions along the filament trajectory are not uniform and, moreover, that anomalous concentrations of tracers of coastal origin (low salinity, many sardine larvae) can persist in the filament for more than half a circuit of the eddy. Whether the anomalous region would have become reintegrated into the coastal upwelling regime remains open to speculation, but the possibility exists that a significant proportion of the offshore flow in the filament is returned intact to the coastal zone. If so then both the net exchange velocity and the horizontal mixing coefficient would be reduced.

As well as horizontal exchanges, there may be vertical ones additional to coastal and eddy upwelling. Evidence has been found in the California Current region that subduction is a feature of filaments (Flament, Armi, & Washburn, 1985; Abbot, Brink, Booth, Blasco, Codispoti, Niiler, & Ramp, 1990). Drifters moving along a filament approached the temperature front defining its southern boundary at a rate that indicated a downwelling velocity of 10 m d^{-1} (Brink, & Cowles, 1991). Chlorophyll and Radon distributions also indicated that waters originating from the near-shore euphotic zone were found at depth offshore, implying similar downwelling rates (Kadko, Washburn, & Jones, 1991; Washburn, Kadko, Jones, Hayward, Kosro, Stanton, Ramp, & Cowles, 1991). However, conflicting conclusions on the location of downwelling emphasise the difficulty in generalising the nature, causes and permanency of subduction. In the present case of the Canaries region, although chlorophyll

structure across the filament was reconcilable with sinking of surface waters, it could equally have arisen from horizontal advection. There is no clear evidence in the present data set to suggest that subduction is a significant feature of the Cabo Bojador filament.

The physical structure of the eddy and filament system exerts a major influence on the strong chemical and biological contrasts between the subtropical oligotrophic waters of the oceanic gyre and the fertile upwelling zone of the eastern boundary. Table 1 summarises this contrast as documented by the work reported in this paper. The most basic biological effects of the northwest African upwelling appear in a number of ways. Isopycnals, and nutrient isopleths, are elevated over a distance of several hundred kilometres from the coast (e.g. Figs. 6 and 17). The result of this tilt, and of weak shoreward flows along the isopycnals, is to bring into the euphotic zone water richer in nutrients than at corresponding depths in the far field, and hence to sustain a greater primary production in a shallower DCM than in the far field. The increased production results in the accumulation of extra phytoplankton, and thus of high concentrations of chlorophyll (e.g. Fig. 6). The increased nutrient fluxes do not, however, seem to perturb the structure of the phytoplankton community, which remains dominated by small organisms, especially phytoflagellates (Kennaway, & Tett, 1994) and prochlorophytes (van Lenning et al., personal communication).

Upwelling takes place in a coastal zone about 50 km wide, corresponding roughly to the continental shelf north of Cabo Bojador. Here there are substantial vertical velocities, averaging 3 m d^{-1} and a maximum of 6 m d^{-1} according to calculated Ekman transport. The mean velocity implies a nitrate flux of $\sim 15 \text{ mmol N m}^{-2} \text{ d}^{-1}$

Table 1

Comparison of typical conditions in oligotrophic waters northwest of the archipelago with those in the African coastal upwelling at 27°N . SML is surface mixed layer. DCM is deep chlorophyll maximum

	Oligotrophic	Coastal upwelling
Nutrients	SML strongly depleted in nitrate; SML up to $4 \mu\text{M}$ nitrate; nitrocline deep.	nitrocline shallow.
Chlorophyll	$< 0.05 \text{ mg chl m}^{-3}$ in SML, DCM of $0(0.1) \text{ mg chl m}^{-3}$ at C. IOOm.	$2-4 \text{ mg chl m}^{-3}$ in SML, no DCM
Production and respiration	Production low, $0.1 \text{ g C m}^{-2} \text{ d}^{-1}$; Mean production high, up to $1 \text{ g C m}^{-2} \text{ d}^{-1}$; respiration high relative to production	respiration low relative to production
Phytoplankton	Typically dominated by cyanobacteria in SML, prochlorophytes and small ($< 5 \mu\text{m}$) phytoflagellates in DCM.	Typically dominated by diatoms and larger ($> 5 \mu\text{m}$) phytoflagellates
Zooplankton and fish larvae	Zooplankton scarce ($0.1 \text{ g protein m}^{-2}$ or less); fish larvae uncommon.	Zooplankton patchily abundant (can exceed $1 \text{ g protein m}^{-2}$):patchily abundant sardine larvae.

into the euphotic zone, explaining surface concentrations up to $4 \mu\text{M}$ seen close to shore and potentially supporting new production of $1 \text{ g C m}^{-2} \text{ d}^{-1}$, similar to the maximum rates measured by ^{14}C assimilation during August 1993. Despite the relatively low ratio (about 2:5) of dissolved silica to nitrate, the flux gave rise to large populations of diatoms as well as large ($> 5 \mu\text{m}$) phytoflagellates, which rapidly assimilated the upwelled nutrients. The result is that superficial concentrations of nutrients fall rapidly with distance from the upwelling centre. Data for HPLC-analysed photosynthetic pigments (van Lenning et al., personal communication), as well as some microscopical observations (Kennaway, & Tett, 1994), suggest that the diatoms rapidly vanish as water enters a filament, although it is unclear whether this is the result of grazing or of sedimentation. The phytoflagellate component (which included cryptomonads) appeared more persistent in August 1993, but it seems gradually to give way to the ‘oligotrophic’ association of small phytoflagellates and cyanobacteria.

The mean flow of the upwelled water has an offshore component in the surface Ekman layer, roughly balanced by a mean shoreward transport at depths below the pycnocline. Given the mean winds during the August cruise of 10 m s^{-1} , the calculated Ekman transport was around $1.8 \text{ m}^2 \text{ s}^{-1}$. However, the actual form of the offshore transport is dominated by the meandering flow around the eddy and by meso-scale mixing processes along its boundaries with oceanic waters (Fig. 23a). As seen in Figs. 11, 12 and 15 the offshore flowing part of the circulation is characterised by a clearly-defined filament of cold water, while the return flow is less evident in sea surface temperature distributions because the surface water has been warmed by insolation to much the same temperature as its surroundings. The horizontal shear between the filament current jet and the surrounding waters results in eddying on a scale of 20 km and smaller (eddy like structures on these scales are seen in Figs. 11 and 12); in this way, an exchange of water parcels between the coastally upwelled water advected in the filament and oceanic waters is effected. Upwelled water is thus entrained into the flow of the Canaries Current and therefore the ocean gyre. As documented earlier, the mesoscale stirring action of the islands of the Canaries archipelago increases the entrainment rate, diverting some of the water from the filament into island-generated eddies which are themselves carried away by the flow of the Canaries Current.

In addition to these horizontal mixing processes, which increase the exchange between oceanic and shelf waters, the Canaries region is also responsible for an increase in the vertical exchange between the nutrient-depleted surface zone and the waters of the upper part of the permanent thermocline, which are moderately rich in nutrients (Fig. 24). The increased vertical exchange is the result of pumping by cold-core eddies as well as upwelling (Table 2). Although the values in this table are preliminary and approximate estimates, they suggest that high vertical velocities in the eddies give rise to nutrient fluxes, which are more important than implied by the area of the eddies themselves. Two estimates are included for the cold-core eddy. One, based on the vertical velocity estimated from the drifter separation from the eddy centre, indicates that potentially the eddy could be as important as the coastal upwelling, whereas a more conservative estimate, assuming a vertical velocity similar

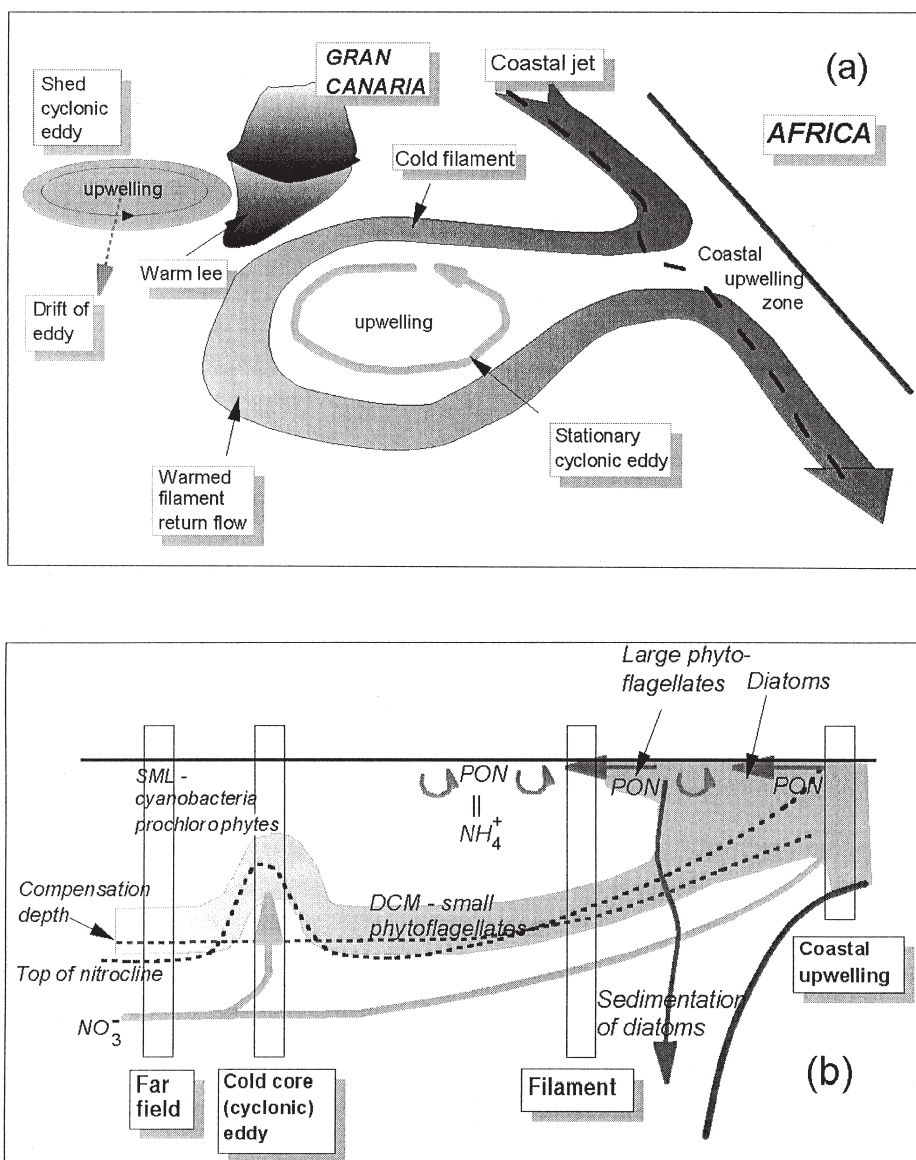


Fig. 24. (a) Schematic of upwelling filament and eddy and (b) associated vertical processes in the filament eddy system. Vertical rectangles indicate typical situations. The *Far-field* nitrocline lies below the compensation depth for phytoplankton growth, and so production is low, carried out by pico- or nanoplankton and likely sustained by recycled ammonium. *Cyclonic Eddies* lift isopycnals and nitrocline relative to the compensation depth, so locally stimulating new production. The DCM intensifies toward the coast and higher nitrate concentrations are exposed above the compensation depth (which itself shallows by shading by more abundant phytoplankton). In the *Upwelling* region, the nitrocline reaches the surface mixed layer, resulting in high production of diatoms, converting nitrate into Particulate Organic Nitrogen. These diatoms sediment or are eaten as upwelled water moves offshore in the *Filament*, leaving large phytoflagellates as the dominant producers, supported by recycled ammonia.

Table 2
Nutrient fluxes related to upwelling filaments and eddies

Category	% Area	Upwelling						Vertical Mixing	Total
		m d ⁻¹	S µM NO ₃	N flux mol m ² yr ⁻¹	Kz m ² d ⁻¹	ΔS/ΔZ mol m ⁴ m ² yr ⁻¹	N flux mol m ² yr ⁻¹		
[0]			[1]				[2]		
Land (Africa)	4%	x	x	x	x	x	x	x	x
Land (Canaries)	2%	x	x	x	x	x	x	x	x
NW African	4%	[3]	3	5	5.5	100	0.01	0.37	67
coastal upwelling									
Filaments	3%	[4]	0	2	0	10	0.08	0.29	2
Permanent	4%	[5]	1	3	1.1	10	0.07	0.26	15
cyclonic eddy in									
coastal trough									
Island generated	1%	[6]	40	{7.5}	22	29.27.3	10	0.08	0.29
wakes and									
cyclonic eddies									
Unperturbed	81%	[7]	0	0	0	1	0.05	0.02	4
oceanic waters									
and anticyclonic									
eddies									

Total area 100% = 285,000 km² Total N flux 173 {111}

[0] Fluxes calculated for 26°–30°N, 13°–19°W. Area of each feature is its typical extent during cruises and as seen in remote sensing.

[1] Nitrate concentrations observed at base of euphotic zone in August 1993.

[2] Nitrate gradients observed in upper thermocline, or at bases of euphotic zone, in August 1993.

[3] Upwelling velocity from estimated Ekman transport (wind stress divergence) averaged over year.

[4] Vertical mixing enhanced by current shear, value estimated.

[5] Upwelling assumed in balance with vertical mixing of heat over upper 50 m (mixing estimated).

[6] Upwelling velocity from radial velocities in eddy observed in August 1993 and from Ekman pumping in lee.

[7] Typical value of eddy diffusion in upper ocean thermocline.

to that caused by the Ekman pumping on the wake boundaries, still shows eddies may be providing a major contribution to the nitrogen flux. The significant result is that the island induced eddies may constitute major components of the flux. Questions of intermittency and intensity of the eddies during the annual cycle remain to be resolved before reliable conclusions may be drawn (Fig. 24).

What is the fate of the nutrients in these enhanced vertical fluxes? The rapid disappearance of diatoms from filaments suggests that some rapidly sink into deeper waters. However, the enhanced chlorophyll concentrations observed in filaments and cyclonic eddies suggests that some of the nutrient is recycled within the euphotic layer, supporting the small-celled phytoplankton seen in these regions. Furthermore, there is evidence from our measurements of ETS activity and ^{14}C uptake in August 1993 (Fig. 25), that respiration was, proportionally, more important in warmer waters. We thus conclude that the regions of strong vertical nutrient flux support enhanced new production of organic matter which is then spread into surrounding, more oligotrophic, waters. As this happens, the enhanced organic carbon (OC) supply supports additional microbial respiration, and the nitrogen in the extra particulate organic nitrogen (PON) may be recycled several times through ammonium. The balance between observed ETS activity and radiocarbon uptake at a given site will

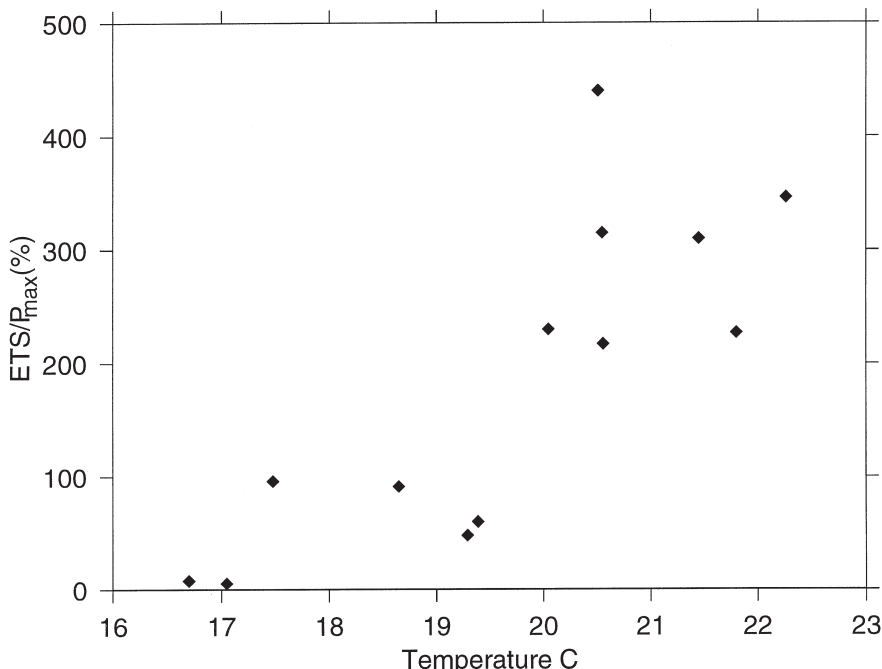


Fig. 25. Relative respiration increase with water temperature at stations in the filament region. Warmer, oligotrophic waters may be net consumers of organic matter produced in upwelling waters. ETS activity represents potential microplankton respiration and was converted to carbon units using a respiratory quotient. Maximum photosynthetic rates (P_{\max}) were taken from Photosynthesis-Irradiance curves determined from ^{14}C experiments in subsamples of the same water as ETS activity.

depend on (a) the supply of OC relative to ammonium and nitrate (DIN), and (b) the effect of these OC and DIN supplies on the relationship between respiration and ETS activity, and between photosynthesis and radiocarbon uptake. It is because these are complex matters that the data in Fig. 24 should not be literally interpreted as showing a shift from an absolute excess of photosynthesis over respiration in upwelling waters, to an absolute excess of consumption over production in warmer waters. Nevertheless, we do suggest that filament transport of organic matter may be more important than their transport of inorganic nutrients.

Finally, we can put the vertical fluxes in Table 2 into a larger perspective. The global input of new nitrogen to the upper ocean from deeper waters is currently estimated as about 85×10^9 kmol y^{-1} (Schlesinger, 1997). We estimate that the total vertical flux in the Canaries region is 0.17×10^9 kmol y^{-1} , or 0.2% of the global total from a sea area which is 0.07% of the world ocean. The Canaries region is thus three times as active in vertical transport of nitrogen as the mean of the global ocean. Most impressive of all, a large part of the vertical flux in the Canaries region occurs in the island-generated eddies, which occupy only about 1% of the area of the region. Their vertical flux, estimated by us at $29 \text{ mol N m}^{-2} \text{ y}^{-1}$, is more than a hundred times the oceanic mean of $0.24 \text{ mol N m}^{-2} \text{ y}^{-1}$.

The Canary islands are efficient suppliers of nutrient to the euphotic zone for a combination of reasons. First, they lie in oligotrophic waters, so the upper-ocean nutrient gradient is relatively large. Second, they are situated in a region of strong atmospheric and oceanic flows, which encourage the formation of energetic eddies with high core upwelling speeds. Third, the eddies can tap relatively high nutrient concentrations because of the regional uplift of the oceanic nitrocline which is associated with the NW African upwelling.

6. Acknowledgements

This work was supported by the MAST programme of the European Commission through Projects 0031 and CANIGO and by the Spanish Consejo Interministerial de Ciencia y Tecnología with provision of ship time and through the FRENTEs project (CICYT, AMB 95-0731). We express our gratitude to our many colleagues who participated in the field work and data processing.

7. References

- Abbot, M.R., Brink, K.H., Booth, C.R., Blasco, D., Codispoti, L.A., Niiler, P.P., & Ramp, S.R. (1990). Observations of phytoplankton and nutrients from a Lagrangian drifter off northern California. *Journal of Geophysical Research*, 95, 9393–9409.
- Arístegui, J. (1990). La distribución de la clorofila *a* en aguas de Canarias. *Boletín del Instituto Español de Oceanografía*, 6(2), 61–72.
- Arístegui, J., Hernández-León, S., Gómez, M., Medina, L., Ojeda, A., & Torres, S. (1989). Influence of the north Trade winds on the biomass and production of neritic plankton in Gran Canaria. In *Topics in Marine Biology*, J.D. Ros, editor. *Scientia Marina*, 53, 223–229.

- Arístegui, J., Sangrá, P., Hernández-León, S., Cantón, M., Hernández-Guerra, A., & Kerling, J.L. (1994). Island-induced eddies in the Canary Islands. *Deep-Sea Research I*, 41, 1509–1525.
- Arístegui, J., Tett, P., Hernández-Guerra, A., Basterretxea, G., Montero, M.F., Wild, K., Sangrá, P., Hernández-León, S., Cantón, M., García Braun, J.A., Pacheco, M., & Barton, E.D. (1997). The influence of island generated eddies on chlorophyll distribution: a study of mesoscale variation around Gran Canaria. *Deep-Sea Research I*, 44, 71–96.
- Bakun, A., & Nelson, C.S. (1991). The seasonal cycle of wind-stress curl in subtropical eastern boundary current regions. *Journal of Physical Oceanography*, 21(12), 1815–1834.
- Ballesteros, S. (1992). *Ignat Pavlyuchenkov cruise report: micro-organisms abundance and distribution*. Data Report 0031-10, School of Ocean Sciences, University of Wales, Bangor, UK.
- Ballesteros, S. (1994). *Influencia de las estructuras mesoscales sobre la distribución y abundancia de bacterias y cianobacterias en aguas de Canarias*. Doctoral thesis. University de Las Palmas de Gran Canaria, 153 pp.
- Barton, E.D. (1994a). Frontal structures downwind and downstream of Gran Canaria. *Annales Geophysicae*, 12, Suppl. II, C267.
- Barton, E.D. (1994b). *European Coastal Transition Zone: Islas Canarias*. Final Report, MAST Project 0031, School of Ocean Sciences, University of Wales, Bangor, UK, 90 pp.
- Basterretxea, G. (1994). *Influencia de las estructuras oceanográficas mesoscales sobre la producción primaria en la región Canaria*. Doctoral thesis, University of Las Palmas de Gran Canaria, 113 pp.
- Braun, J.G. (1980). Estudios de producción en aguas de las Islas Canarias. I, hidrografía, nutrientes y producción primaria. *Boletín del Instituto Español de Oceanografía*, 285, 149–154.
- Braun, J.G., & Escáñez, J.E. (1996). *Distribution of nutrients and dissolved oxygen during the Ignat Pavlyuchenkov cruise (October 1991)*. Data Report 0031-18, School of Ocean Sciences, University of Wales, Bangor, UK.
- Braun, J.G., Orzaiz, I., Armas, J.D., & Real, F. (1985). Productividad y biomasa del ultraplanton, nanoplanton y fitoplanton de red en aguas de las Islas Canarias. *Boletín del Instituto Español de Oceanografía*, 2(1), 192–204.
- Brink, K.H., & Cowles, T.J. (1991). The Coastal Transition Zone Experiment. *Journal of Geophysical Research*, 96, 14637–14647.
- Castagné, N., Le Borgne, P., Le Vourch, J., & Olry, J.P. (1986). Operation measurement of sea surface temperatures at CMS Lannion from NOAA-7 AVHRR data. *International Journal of Remote Sensing*, 7, 953–984.
- De León, A.R., & Braun, J.G. (1973). Ciclo anual de la producción primaria y su relación con los nutrientes en aguas Canarias. *Boletín del Instituto Español de Oceanografía*, 167, 1–24.
- Flament, P., Armi, L., & Washburn, L. (1985). The evolving structure of an upwelling filament. *Journal of Geophysical Research*, 90, 11765–11778.
- Hagen, E., Zülicke, C., & Feistel, R. (1996). Near-surface structures in the Cape Ghir filament off Morocco. *Oceanologica Acta*, 19(6), 577–598.
- Haynes, R., Barton, E.D., & Pilling, I. (1993). Development, persistence, and variability of upwelling filaments off the Atlantic coast of the Iberian Peninsula. *Journal of Geophysical Research*, 98, 22681–22692.
- Hayward, T.L., & Mantyla, A.W. (1990). Physical, chemical and biological structure of a coastal eddy near Cape Mendocino. *Journal of Marine Research*, 48, 825–850.
- Hernández-Guerra, A., Arístegui, J., Cantón, M., & Nykjaer, L. (1993). Phytoplankton pigment patterns in the Canary Islands as determined using Coastal Zone Colour Scanner data. *International Journal of Remote Sensing*, 14, 1431–1437.
- Hernández-León, S. (1988). Gradients of mesozooplankton biomass and ETS activity in the wind shear area as evidence of an island mass effect. *Marine Biology*, 10, 1141–1437.
- Hernández-León, S. (1991). Accumulation of mesozooplankton in a wake area as a causative mechanism of the ‘island mass effect’. *Marine Biology*, 109, 141–147.
- Hill, A.E., Hickey, B.M., Shillington, F.A., Strub, P.T., Brink, K.H., Barton, E.D., & Thomas, A.C. (1997). Eastern Ocean Boundaries. In: *The Sea*, A.R. Robinson and K.H. Brink (editors), 10,
- Huyer, A., Kosro, P.M., Fleischbein, J., Ramp, S.R., Stanton, T., Washburn, L., Chavez, F.P., Cowles,

- T.J., Pierce, S., & Smith, R.L. (1991). Currents and water masses of the Coastal Transition Zone off Northern California, June to August 1988. *Journal of Geophysical Research*, 96, 14809–14832.
- Huyer, A., & Kosro, P.M. (1987). Mesoscale surveys over the shelf and slope in the upwelling region near Point Arena. *California, Journal of Geophysical Research*, 92, 1655–1681.
- Ikeda, M., & Emery, W.J. (1984). Satellite observations and modelling of meanders in the California Current System off Oregon and northern California. *Journal of Physical Oceanography*, 14, 3–12.
- Jones, B.D., Mooers, C.N.K., Rienecker, M.M., Stanton, T., & Washburn, L. (1991). Chemical and biological structure and transport of a cool filament associated with a jet-eddy system off northern California in July 1986 (OPTOMA 21). *Journal of Geophysical Research*, 96, 22207–22225.
- Kadko, D.C., Washburn, L., & Jones, B. (1991). Evidence of subduction within cold filaments of the northern Californian coastal transition zone. *Journal of Geophysical Research*, 96, 14909–14926.
- Kennaway, G.M., & Tett, P. (1994). *A scanning electron microscope study of flagellate assemblies from the Hespérides Cruise 9308*. Data Report 0031-17, School of Ocean Sciences, University of Wales, Bangor, UK.
- Kostianoy, A.G., & Zatsepin, A.G. (1996). The West African coastal upwelling filaments and cross-frontal water exchange conditioned by them. *Journal of Marine Systems*, 7, 349–359.
- La Violette, P.E. (1974). A satellite-aircraft thermal study of the upwelled waters off Spanish Sahara. *Journal of Physical Oceanography*, 4, 676–685.
- Le Borgne, P., Le Vourch, J., & Marsouin, A. (1988). Sea surface temperature parameters inferred from meteorological satellite data at CMS Lannion. *International Journal of Remote Sensing*, 9, 1819–1834.
- Li, W.K.W. (1994). Primary production of prochlorophytes, cyanobacteria, and eukaryotic ultraphytoplankton—measurements from flow cytometric sorting. *Limnology and Oceanography*, 39, 169–175.
- Lutjeharms, J.R.E., & Stockton, P.L. (1987). Kinematics of the upwelling front off southern Africa. *South African Journal of Marine Science*, 5, 35–50.
- Montero, M.F. (1992). *Ignat Pavlyuchenkov cruise report: Electron Transport System Activity (ETS) in microplankton around the Canary Islands*. Data Report 0031-11, School of Ocean Sciences, University of Wales, Bangor, UK.
- Montero, M.F. (1993). *Respiración y actividad ETS en microplancton marino. Variabilidad del ETS en aguas de Canarias*. Doctoral thesis, University of Las Palmas de Gran Canaria, 194 pp.
- Mooers, C.N.K., & Robinson, A.R. (1984). Turbulent jets and eddies in the California Current and inferred cross-shore transports. *Science*, 223, 51–53.
- Navarro-Pérez, E. (1996). *Physical oceanography of the Canary Current: short term, seasonal and interannual variability*. Doctoral Thesis, Univ. of Wales, Bangor, 160 pp.
- Navarro-Pérez, E., Vélez-Muñoz, H.S., & Wild, K.A. (1994). *BIO Hespérides Cruise 9308 Cruise Report: Hydrographic Fields*. Data Report 0031-16, School of Ocean Sciences, University of Wales, Bangor, UK.
- Navarro-Pérez, E., & Barton, E.D. (1995). *BIO Hespérides Cruise 9308 Cruise Report: Acoustic Doppler Current Fields*. Data Report 0031-19, School of Ocean Sciences, University of Wales, Bangor, UK.
- Nykjaer, L., & Van Camp, L. (1994). Seasonal and interannual variability of coastal upwelling along northwest Africa and Portugal from 1981 to 1991. *Journal of Geophysical Research*, 99, 14197–14208.
- Ramp, S.R., Jessen, P.F., Brink, K.H., Niiler, P.P., Daggett, F.L., & Best, J.S. (1991). The physical structure of cold filaments near Point Arena, California, during June 1987. *Journal of Geophysical Research*, 96, 14859–14884.
- Rodríguez, J.M. (1996). *El ictioplancton en la Región Canaria: abundancia, distribución y composición taxonómica larvaria*. Doctoral thesis, University of La Laguna, Tenerife, 209 pp.
- Roy, C. and Mendelsohn R. (1995). *Comprehensive Ocean Dataset Extraction users guide*. Climate and Eastern Ocean Systems project report, 62 pp.
- Sangrá, P. (1995). *Perturbación de un flujo geofísico por un obstáculo: aplicación a la isla de Gran Canaria*. Doctoral thesis, University of Las Palmas de Gran Canaria, 200 pp.
- Schlesinger, W.H. (1997). Biogeochemistry. Analysis of global change (2nd Edition). Harcourt Brace Jovanovich, San Diego, 433 pp.
- Shapiro, G., Barton, E.D., & Meschanov, S.L. (1997). Capture and release of Lagrangian floats by eddies in shear flow. *Journal of Geophysical Research*, 102, 27887–27902.

- Speth, P., Detlefsen, H., & Sierts, H.W. (1978). Meteorological influence on upwelling off Northwest Africa. *Deutsches Hydrografisches Zeitschrift*, 31, 95–104.
- Stramma, L., & Siedler, G. (1988). Seasonal changes in the North Atlantic Subtropical Gyre. *Journal of Geophysical Research*, 93, 8111–8118.
- Strub, P.T., Kosro, P.M., & Huyer, A. (1991). The nature of the cold filaments in the California Current System. *Journal of Geophysical Research*, 96, 14743–14768.
- Traganza, E.D., Nestor, D.A., & McDonald, A.K. (1980). Satellite observations of a nutrient upwelling off the coast of California. *Journal of Geophysical Research*, 85, 4101–4106.
- Van Camp, L., Nykjaer, L., Mittelstaedt, E., & Schlittenhardt, P. (1991). Upwelling and boundary circulation off Northwest Africa as depicted by infrared and visible satellite observations. *Progress in Oceanography*, 26, 357–402.
- Vélez-Muñoz, H.S. (1992). *Ignat Pavlyuchenkov cruise report: Hydrographic fields*. Data Report 0031-09, School of Ocean Sciences, University of Wales, Bangor, UK.
- Washburn, L., Kadko, D.C., Jones, B.H., Hayward, T., Kosro, P.M., Stanton, T.P., Ramp, S., & Cowles, T. (1991). Water mass subduction and the transport of phytoplankton in a coastal upwelling system. *Journal of Geophysical Research*, 96, 14927–14945.
- Wild, K.A. (1992). *Ignat Pavlyuchenkov cruise report: general and phytoplankton biomass*. Data Report 0031-08, School of Ocean Sciences, University of Wales, Bangor, UK.
- Wild, K.A. (1995). *The dynamics of the deep chlorophyll maximum in the vicinity of the Canary Islands (Spain)*. Doctoral Thesis, Univ. of Wales, Bangor, 254 pp.
- Wooster, W.S., Bakun, A., & McLain, D.R. (1976). The seasonal upwelling cycle along the eastern boundary of the North Atlantic. *Journal of Marine Research*, 34, 131–141.